Coupling between ribotypic and phenotypic traits of protists across life-cycle stages and temperatures

Songbao Zou[1, 2], Rao Fu[1, 2, 3], Qianqian Zhang[1, 2], Eleni Gentekaki[4], Jun Gong[5, 6*]

[1] *Yantai Institute of Coastal Zone Research, Chinese Academy of Sciences, Yantai, China,*

[2] *University of Chinese Academy of Sciences, Beijing, China,*

[3] *Shandong Institute of Sericulture, Shandong Academy of Agricultural Sciences, Yantai, China,*

[4] *School of Science, Mae Fah Luang University, Chiang Rai, 57100, Thailand,*

[5] *School of Marine Sciences, Sun Yat-Sen University (Zhuhai Campus), Zhuhai, China,*

[6] *Southern Marine Science and Engineering Guangdong Laboratory (Zhuhai), Zhuhai, China*

Correspondence:

Jun Gong, School of Marine Sciences, Sun Yat-sen University, Zhuhai Campus, Tangjiawan, Zhuhai 519082, China, gongj27@mail.sysu.edu.cn

Running title: Coupling ribotypic to phenotypic traits in protists

ABSTRACT

Relationships between ribotypic and phenotypic traits of protists across life-cycle stages remain largely unknown. Herein, we assessed the effect of life-cycle stage (lag, log, plateau, cyst) and temperature on quantity and polymorphisms of ribosomal (r)RNA gene (rDNA) and rRNA transcripts by using single cells of ciliate species. *Colpoda inflata* and *C. steinii* demonstrated allometric relationships between 18S rDNA copy number per cell (CNPC), cell volume (CV), and macronuclear volume across all life-cycle stages. Integrating previously reported data of *Euplotes vannus* and *Strombidium sulcatum* indicated taxon-dependent rDNA CNPC–CV functions. Ciliate and prokaryote data analysis revealed that the rRNA CNPC followed a unified power-law function, only if the rRNA-deficient resting cysts were not considered. Hence, a theoretical framework was proposed to estimate quantity of resting cysts of a protistan population. Using rDNA CNPC was a better predictor of growth rate at a given temperature than rRNA CNPC and CV, suggesting replication of redundant rDNA operons is a key factor that slows cell division. Single-cell high throughput sequencing revealed hundreds to thousands of rDNA and rRNA variants. The number of rDNA variants corresponded to the amount of cellular rDNA. Despite intra-individual divergence reaching up to 9%, operational taxonomic units (OTUs) clustered in a species-specific manner and independently of life-cycle stage or temperature. This indicates limited influence of said divergence on distributional pattern of OTU richness among samples.

IMPORTANCE

Based on phenotypic traits, traditional surveys usually characterize organismal richness, abundance, biomass, and growth potential to describe diversity, organization and function of protistan populations and communities. The ribosomal RNA gene (rDNA) and its transcripts have been widely used as molecular markers in ecological studies of protists. Nevertheless, the manner in which these molecules relate to cellular (organismal) and physiological traits remains poorly understood, which could lead to misinterpretations. The current research supports the idea that cellular ribosomal RNA transcript quantity reflects cell volume (biomass) of protists better than rDNA quantity, across multiple life-cycle stages except for resting cysts. We demonstrate that quantity of resting cysts and maximum growth rate of a population can be theoretically estimated using ribotypic trait-based formulas. Assessment of rDNA and rRNA sequence polymorphisms at

single-cell level indicates that intra-individual divergence does not affect recognizing variational patterns of protistan diversity across time and space.

KEYWORDS: Cell size; Copy number variation; Growth rate; Life-cycle; Ribosome heterogeneity.

INTRODUCTION

Protists are single-celled eukaryotes of astounding morphological and functional diversity inhabiting virtually every life-harboring niche on this planet (Caron et al., 2009). These microorganisms have complex life cycles comprising stages of distinct phenotypic traits (e.g., morphology, cell size and growth rate). Several of these traits undergo changes in response to fluctuating environmental variables (Corliss, 2001; Padilla and Savedo, 2013; Mulot et al., 2017). Cyst formation is a widespread trait among protists and is commonly induced under stressful conditions. Protists can form different types of cysts (e.g., resting, division and unstable cysts), which are typically nonmotile and dormant. Cysts play important roles in the ecology of protists, as they are resistant to unfavorable conditions, e.g., food depletion, overpopulation, drying, temperature and barometric pressure extremes, ultraviolet irradiation, and changing chemical factors (McQuoid and Hobson, 1996; Corliss, 2001; Persson, 2001; Ross and Hallock, 2016). Cyst cells comprise an essential life cycle stage of many protists promoting dispersal to new locations, thus increasing their population in a short period of time (Corliss and Esser, 1974; Corliss, 2001). Protistan diversity, community composition, rare-to-abundant transition, seasonality, biogeographical patterns, dynamic responses to perturbations, as well as, ecological and biogeochemical functions in soil, planktonic and benthic systems are all affected by dormancy of cysts (Corliss, 2001; Persson, 2001; Fistarol et al., 2004; Anderson and Rengefors, 2006), highlighting its functional and ecological significance in natural systems. However, cysts are highly reduced in size and lack most diagnostic morphological features in comparison with vegetative cells. As such, protistan cysts are usually difficult to morphologically identify and enumerate in environmental samples (Corliss, 2001).

The difficulties in morphological identification of protistan species in natural ecosystems have been largely circumvented by metabarcoding analyses using ribosomal (r)RNA genes (rDNA) and/or rRNA transcripts as molecular markers. Nevertheless, recent studies have shown that the number of rDNA copies in protists is highly variable raising concerns in regards to its effect on estimates of species richness and evenness in a community (reviewed in Fu and Gong, 2017). The majority of these investigations have not taken into account variability of rDNA copy number (CN) of various life stages, particularly in the cystic forms. So far, cystic rDNA CN data are only available for a limited number of protistan species, e.g., bloom-forming dinoflagellates (e.g., Erdner

et al., 2010) and medically important amoebae (e.g., Rivière et al., 2006). Hence, fundamental knowledge on cystic rDNA and rRNA transcripts and their effect on taxon richness and evenness is still lacking. Moreover, CN of rRNA (a proxy of ribosome number) in a cyst has seldom been quantified, probably due to the common assumption that rDNA is sparsely or not at all transcribed in the dormant stages. Nevertheless, it has been noted that, apart from phenotypic changes (reduction of cell volume and nuclear size), encystment also induces substantial genetic alterations, including loss of genomic DNA and altered nuclear DNA methylation patterns (Gutiérrez et al., 1998). Previous studies have demonstrated variation in rDNA CN in a foraminiferan species across life cycle stages (Parfrey et al., 2012), and have provided support for scaling relationships among rDNA, rRNA CNs per cell, growth rate, and cell volume (CV) during the exponential growth stage of ciliate species (Fu and Gong, 2017). Collectively considering these data, it is reasonable to expect a substantial decrease of the CNs of both cellular rDNA and rRNA during encystment due to shrinkage of the whole cell. However, the following points have yet to be empirically investigated: (1) the extent to which the ribotypic CNs and their ratios are reduced in cysts; (2) the quantitative relation of these ribotypic traits to phenotypic traits across different growth stages (e.g., lag, log, plateau and cystic phases); and (3) whether previous models of ribotypic CN-CV scaling relationships hold for cysts.

The available data suggest that the rDNA operons of diverse protistan groups have a high degree of intra-individual polymorphisms (Pillet et al., 2012; Gong et al., 2013; Decelle et al., 2014; Weber and Pawlowski, 2014; Kudryavtsev and Gladkikh, 2017; Wang et al., 2017), but the variability of protistan rDNA polymorphisms has rarely been linked to life cycle stages and/or to environmental conditions. Hence, if the cellular rDNA CN oscillates during the life cycle (Parfrey et al., 2012), it is conceivable that some rDNA variants may be differentially eliminated or amplified, resulting in altered ribotypic diversity across developmental stages and variable environmental (e.g., temperature) conditions. More importantly, the intracellular rRNA landscape could be further altered, resulting in ribosomal structural heterogeneity, due to selective transcription of specific rDNA operons, as has been previously shown for several prokaryotes and an apicomplexan protist (e.g., Gunderson et al., 1987; López-López et al., 2007; Genuth and Barna, 2018; Kurylo et al., 2018). However, the dynamics of both rDNA operons and rRNA molecules (ribosomes) within a protistan cell at different life cycle stages or under varying conditions have been little explored.

In this study, we used two ubiquitously distributed soil ciliate species of *Colpoda* to investigate both rDNA and rRNA CNs across lag, log (exponential), plateau (stationary), unstable and resting cyst stages. *Colpoda* has been used as a model for the study of cyst-related biology and ecology for a long time (e.g., Stout, 1955; Gutiérrez et al., 1998; Müller et al., 2010). The two species were reared at two temperatures (18ºC and 28ºC) and their phenotypic features (cell size, macronuclear size, nucleocytoplasmic ratio) were determined. The environmental and growth-stage effects on intra-individual polymorphisms of ribotypic sequences were explored by comparing the distributional patterns and nucleotide contents of rDNA and rRNA variants in actively growing cells vs. resting cysts at both temperatures. We also extended previous work on the marine ciliates *Euplotes vannus* and *Strombidium sulcatum*, which were reared at three different temperatures by analyzing rDNA and rRNA sequence diversity in actively growing cells (Fu and Gong, 2017). Single ciliate cells were used for quantitative PCR and high throughput sequencing of rDNA and rRNA (cDNA). Our main expectations were that: (1) in line with reduction of cell and macronuclear size, the quantity of both rDNA operons and rRNA transcripts would be highly reduced in the cystic forms; (2) the scaling relationships between ribotypic CN and CV would generally hold across life cycle stages; and (3) the intra-individual polymorphic traits of both rDNA operons and rRNA molecules (ribosome composition) would be life stage- and temperature-dependent.

MATERIALS AND METHODS

Source organisms, cultivation and treatments

Two cyst-forming, soil ciliate species, *Colpoda steinii* and *C. inflata*, were collected from a coastal apple orchard in Yantai, Shandong, China. The protists were cultivated and isolated using the non-flooded Petri dish method (Omar et al., 2017). *Euplotes vannus* and *Strombidium sulcatum* were originally isolated from the coastal waters off Qingdao (Shandong, China), and have been maintained in the laboratory for a long time. For the purpose of this study, cultures of these four species were initiated from a single cell supplied with bacterial food.

Cultivation of these ciliates and monitoring of their abundances were as previously described (Fu and Gong, 2017). In brief, ten cells of each species were picked with a micropipette, washed several times to remove other microorganisms, and then inoculated into a tissue-culture flask with 50 ml water. All ciliates were fed with heat-killed *Escherichia coli* (at 70 ℃ for 10 min) cells, which

were cultured in LB-medium, pelleted and resuspended in ~20 ml sterilized water. The *Colpoda* species grew well and underwent distinct phases (lag, log, and plateau) during an incubation period of ten days at 18 ℃ and 28 ℃. Following the plateau phase, both species consistently formed resting cysts, probably due to overpopulation and food depletion. Phase-specific cells (including the resting cysts) were individually isolated to determine both phenotypic and ribotypic traits at the single-cell level. The two marine species *E. vannus* and *S. sulcatum* were reared at 16 ℃, 21 ℃ and 25 ℃. For these two species, only cells in log phase were investigated. In order to explore possible footprint effect of the higher temperature on ribotypic traits, we set an additional "touchdown" treatment (designated with "*") as previously described (Fu and Gong, 2017): briefly, a few individuals of the treatments maintained at 25 ℃ for 30 d were transferred and re-cultured at 16 ℃ for another month. All treatments were done in triplicate.

Many ciliate species become thin-walled, partially dehydrated, and division inhibited when temperature shifts beyond certain limitations in a short time period, thus form unstable cysts (Stout, 1955). These unstable cysts are generally larger than the resting cysts, and undergo complete ciliary dedifferentiation returning to vegetative cells in a few hours. We tried obtaining unstable cysts of *Colpoda* by chilling cells for various periods of time. Tubes containing actively growing vegetative cells were transferred into three separate conditions: ice-water mixture (0 ℃) and chemostats at 4 ℃ and 10 ℃. Twenty μL of culture solution were used to identify and count vegetative cells and unstable cysts, all of which were subsequently observed using a stereomicroscope (XLT-400, Guiguang, China) at 45× magnification. The dynamics of the unstable cysts and vegetative cells were monitored every 0.5 to 2 h to determine the optimal time period for achieving the highest yield of unstable cysts. All chilling treatments were performed in triplicate. Since unstable cysts reflect high phenotypic plasticity, relevant phenotypic and ribotypic traits of this temporary stage were also determined and analyzed.

Determination of growth rate, cell volume and macronuclear size

The cell abundances were determined once a day (Fig. 1A). Growth rates of the two *Colpoda* species were calculated as the slope of *ln* individual versus time during the logarithmic phase. At least 18 cells from each growth stage were randomly selected and fixed with Lugol's solution (final concentration 2%). This fixation approach is identical to the one we previously used for

characterizing cell sizes of *E. vannus* and *S. sulcatum*, and allows direct comparisons of relevant data between studies. The cell width and length were individually measured at 400x magnification using a compound microscope (Olympus BX51, Tokyo, Japan). Fixed vegetative cells of both *Colpoda* species were ellipsoid, with cell thickness approximately equal to cell width. Cell volume (CV) was calculated according to the formula:

$$CV = 4/3 * \pi * (length/2) * (width/2) * (thickness/2).$$

Both resting and unstable cysts were spheroid, thus their length, width and thickness were considered equal.

Macronuclear and cell sizes of two *Colpoda* species were determined based on specimens fixed with Bouin's solution and stained using protargol impregnation (Wilbert, 1975). This approach reveals morphological features of ciliates (e.g., nuclear size, infraciliature) in detail, thus has been commonly used for their identification and taxonomy (Warren et al., 2017). Nevertheless, the fixative may alter the volume of the cells compared with the Lugol's fixation. To circumvent this issue, volumes of both protargol impregnated specimens and those fixed with Lugol's were determined. Measurements of length and width of the cells and their macronuclei were carried out using a compound microscope (Olympus BX51) at a magnification of 1000X. The volumes of oval to ellipsoidal cells and macronuclei were calculated as above described.

Cell lysis, DNA extraction and cDNA synthesis

Cell lysis, DNA extraction and RNA transcription of single-cells followed Fu and Gong (2017). In brief, ciliate cells/cysts were picked and washed with autoclaved double distilled water. A single cell with a minimum amount of water was then transferred with a micropipette into the inner wall surface of a nuclease-free PCR tube. This process was carried out for more than 18 cells per stage. Before adding lysis solution, cell presence was verified using a stereoscope. Only tubes with intact cells were kept. Tubes containing broken cells were discarded to minimize RNA degradation. Cell lysis and nucleic acid extraction were performed for all 18 replicates on an ultra-clean bench pre-treated with RNaseZap (Ambion). Each cell was suspended in 1 μL of distilled water, with addition of 2 μL of mixed solution containing 1.9 μL 0.2% Triton-X-100 (Solarbio, Beijing, China) and 0.1 μL of recombinant RNase inhibitor (Takara, Biomedicals, Japan). The tubes were gently flicked and centrifuged briefly, then incubated at room temperature for 10 min. Nuclease-free PCR

tubes, microtubes and micropippette tips (Axygen Scientific, CA, USA) were used for all manipulations. One μL of the cell suspension was used to extract genomic DNA, while 2 μL were used for RNA reverse transcription. Genomic DNA extraction was performed with a REDExtract-N-Amp Tissue PCR Kit (Sigma, St. Louis, MO), according to the manufacturer's instructions, except the suggested volume of each reagent was modified to 1/50, as previously described (Gong et al., 2014).

The RNA reverse transcription of single cells was as previously described (Fu and Gong, 2017). The remaining 2 μL of cell suspension were mixed with 1 μL random hexamers B0043 (10 μM, Sangon, China) and 1 μL of dNTP mix (10 μM). After incubation at 72 ℃ for 3 min the tube was immediately transferred onto ice. RNA was reverse transcribed using a SuperScript III Reverse Transcriptase Kit (Invitrogen, CA, USA). The total volume used for PCR was 12.42 μL, which was made up of 4 μL rRNA template, 3 μL 5× first strand buffer, 0.3 μL SuperScript III reverse transcriptase, 1 μL 0.1M DTT, 2 μL Betaine (Sigma–Aldrich), 0.12 μL 0.5M $MgCl_2$, 1 μL RNase inhibitor (Roche, Germany), and 1 μL DEPC-treated water. The following program was run on a thermal cycler (Biometra, Gottingen, Germany): an initial temperature of 50 ℃ for 90 min, followed by 10 cycles at 55 ℃ for 2 min, with a final step at 70 ℃ for 15 min. Both the DNA and synthesized cDNA were stored at -80 ℃ for subsequent assays.

Quantitative real-time PCR (qPCR)

For quantifying 18S rDNA and rRNA (cDNA) copy numbers in *Colpoda* cells, the newly designed species-specific primers CsQ207f (5'-TAACCCTGGCAACAGGA-3') and CsQ459r (5'-TGCAATCTCGCAACCCCA-3') were used in qPCR assays to amplify a 252-bp fragment of the 18S rRNA gene of *C. steinii*. The eukaryote-specific primers EUK345f (5'-AAGGAAGGCAGCAGGCG-3') and EUK499r (5'-CACCAGACTTGCCCTCYAAT-3') (Zhu et al., 2005) were used to amplify a 149-bp fragment of *C. inflata*. Two standard curves were constructed with the sequences of the two *Colpoda* species as previously described by Gong et al. (2013). In brief, serial 10-fold dilutions (10^{-3} to 10^{-10}) were used to generate the standard curves. The qPCR reaction was performed using SYBR Premix Ex Taq™ II (Takara, Dalian, China). The reaction solution (20 μL) contained 0.4 μL of 10 μM primers, 0.4 μL ROX Reference Dye II, 10 μL Premix Ex Taq II, 7.8 μL milli-Q water and 1 μL template. All the qPCR reactions were performed

on a 7500 Fast Real-Time PCR System (Applied Biosystems) with the following program: 95 ℃ for 7 min, followed by 45 cycles of 95 ℃ for 30 s, 55 ℃ (60 ℃ for *C. inflata*) for 1 min, and 72 ℃ for 1 min (77 ℃ for 25 s for *C. inflata*). The data were collected at 72 ℃ and 77 ℃ for *C. steinii* and *C. inflata*, respectively; all reactions ended with a melt curve stage from 60 ℃ to 95 ℃ (gradually increasing by 0.3 ℃). Standard curves were generated using $\log_{10}$ number of copies vs. the threshold cycle (Ct). The linear correlation coefficient (R^2) ranged from 0.997 to 1.000. The amplification efficiency ranged from 99% to 103%. As the samples of rRNA also contained genomic rDNA, the rRNA (cDNA) copy numbers were calculated by subtracting the rDNA CNs from the sum of rDNA and cDNA copy numbers.

Single-cell high throughput sequencing

Genomic DNA and synthesized cDNA from single cells of each of the four ciliate species was used for high throughput sequencing. These included cells of *Colpoda steinii* and *C. inflata* at two typical stages (i.e., vegetative cells in log-phase and resting cysts) and under two temperatures (18 ℃ and 28 ℃), plus *Euplotes vannus* and *Strombidium sulcatum* during log phase grown at four temperature treatments (i.e., 16 ℃, 21 ℃, 25 ℃ and 16* ℃; Fu and Gong, 2017). In the samples for cDNA sequencing, genomic DNA was completely digested at 37 ℃ for 1 h using a TURBO DNA-free Reagent Kit (Invitrogen), in which the digestion mixture consisted of 1 μl cell lysate, 1 μl 10×TURBO DNase buffer, 1 μl TURBO DNase (2 units μl^{-1}), and 7 μl nuclease-free water.

The V4 hypervariable regions of 18S rDNA and cDNA in *C. steinii* and *C. inflata* were amplified with the eukaryotic specific primers TAReuk454FWD1 (5'-CCAGCASCYGCGGTAATTCC-3'), TAReukREV3 (5'-ACTTTCGTTCTTGATYRA-3') (Stoeck et al., 2010). The V1-V3 regions of 18S rDNA and cDNA in *E. vannus* and *S. sulcatum* were amplified with primers Euk82F (5'-GAADCTGYGAAYGGCTC-3') and Euk516R (5'-ACCAGACTTGCCCTCC-3') (Díez et al., 2001; Dawson and Pace, 2002). A 6-bp barcode was added to the sequences of the forward and reverse primers aimed to identifying each sample. The PCR reaction solution (30 μL) contained 10 ng of DNA or cDNA, 0.2 μM of each primer, and 15 μL of 2× Phusion High-Fidelity PCR Master Mix (New England Biolabs). All PCR amplification reactions were carried out on a T100 Thermal Cycle (Bio-Rad) with the following program: an initial pre-denaturation at 98 ℃ for 1 min, followed by 30 cycles of denaturation at 98 ℃ for 10 s,

annealing at 50 ℃ (56 ℃ for two marine ciliates) for 30 s, and elongation at 72 ℃ for 30 s, with a final extension step of 72 ℃ for 5 min. The libraries were prepared using a NEB Next Ultra DNA Library Prep kit. Paired-end 250 bp and 300 bp sequencing was executed on HiSeq and MiSeq platforms (Illumnina, USA) for the soil and marine species, respectively. A total of 80 single-cell rDNA and rRNA pools of the two *Colpoda* species were sequenced. For each *Colpoda*, 20 cells were used to sequence DNA and another 20 for cDNA. There were five biological replicates for each treatment. Four samples failed to be amplified, resulting in 39 samples of logarithmic phase and 37 samples of resting cysts. A total of 48 single cells of *E. vannus* and *S. sulcatum* were sequenced. For each species, 24 cells were used to sequence DNA and 24 for RNA pools. Each treatment was run in triplicate.

Data processing and analysis

A total of 8,478,407 reads were generated for rDNA and cDNA of the four ciliate species (Table S1). Data processing and analysis was done using a combination of Prinseq-lite v.0.20.4 (Schmieder and Edwards, 2011), QIIME v.1.8.0 (Caporaso et al., 2010) and MOTHUR v.1.34.4 (Schloss et al., 2009). Quality control was conducted and high-quality reads were retained according to the following criteria: length of the reads including primers and barcode sequences ≥ 380 and ≥ 400 bp for the soil and marine species, respectively; quality score > 20; no ambiguous bases; no primer sequence mismatches; and homopolymers ≤ 6. Reads of replicates of the same species were merged in a single file. USEARCH v.61 was used to screen for putative chimeras (Edgar, 2010) based on Silva database (release 132). Primer sequences were trimmed off and amplicons were assigned to their closest hits in the Silva database using UCLUST v.1.2.2 (Edgar, 2010) with a minimum 90% identity threshold. Based on taxonomic assignment, the reads assigned to each species were extracted by MOTHUR. Singletons (the unique variants with a single read across all samples of the same species) were excluded prior to further analysis. For treatments of each species, the filtered reads were clustered using UCLUST at various similarity thresholds ranging from 90% to 100%, and ribotypic polymorphisms between rDNA and rRNA sequences and across treatments were assessed.

Characterizations of single-cell ribotype sequence polymorphisms

Nucleotide polymorphisms were identified by aligning all rDNA and rRNA (cDNA) reads against the dominant haplotype of each species, which was implemented using Burrows-Wheeler Aligner v.0.7.17 with default parameters (Li and Durbin, 2009). The alignments were converted into BAM format, sorted and indexed using SAMtools v.0.1.19 (Li et al., 2009). The ribotype nucleotide polymorphisms of each species were then called using the *mpileup* function and summarized using an in-house *perl* script (printBasesBwa2.pl).

Statistical analysis

Student's *t*-test (two-tailed) was performed to test the significance (α = 0.05) of the growth phase-wise differences in phenotypic (i.e., cell volume, macronuclear volume, cell to macronuclear volume ratio) and ribotypic traits (per-cell rDNA and rRNA CNs and concentrations, rDNA: rRNA CN ratio). The maximum growth rates of two *Colpoda* species at two different temperatures were also statistically compared using *t*-test. Pearson correlation and linear regression analyses were carried out to link these phenotypic traits with ribotypic traits or to explore the association between ribotypic traits. All these analyses were executed using the statistical software SPSS v.13.0 (SPSS, Chicago, IL).

Nucleotide sequence accession numbers

The reads from the high throughput sequencing of eukaryotic 18S rRNA genes and transcripts are available under accession numbers SRR10589967 - SRR10590042 (*Colpoda steinii* and *Colpoda inflata*) and SRR10590394 - SRR10590441 (*Euplotes vannus* and *Strombidium sulcatum*).

RESULTS

Cell volume, macronuclear volume, and nucleocytoplasmic ratio

The lag, logarithmic, plateau and resting cystic phase of *Colpoda steinii* and *C. inflata* were distinguishable when cultured with replete bacterial prey at both 18 ℃ and 28 ℃ (Fig. 1A). At 28 ℃, the two species grew approximately 2 and 6 times faster than at the 18 ℃ treatments, respectively. At both temperatures, the smaller species (*C. steinii*) grew consistently faster than the larger species (*C. inflata*): 7.2 ± 0.87 d^{-1} (mean ± SE) vs. 5.1 ± 0.09 d^{-1} at 28 ℃, and 3.6 ± 0.32 d^{-1} vs. 0.9 ± 0.32

d^{-1} at 18 ℃ (Fig. 1B). Abundant unstable cysts were successfully obtained by chilling actively growing cells of *C. steinii* at 0 ℃ for 4 h and *C. inflata* at 4 ℃ for 10 h (Fig. S1).

The cell volume (CV) of both *Colpoda* species progressively reduced through lag, log, and plateau to resting cyst phases at both temperatures (Fig. 1C, D; 2A). In the 18 ℃ treatment of *C. inflata*, the largest CV (about 2.14×10^5 μm^3) was recorded for the lag phase cells. Upon entering the exponential phase, the cells became smaller (on average 8.9×10^4 μm^3), and further shrank by 46% in plateau phase to about 4.8×10^4 μm^3. Relative to the log-phase cells, the resting cysts of this species greatly reduced by 83% in size to 1.5×10^4 μm^3. *Colpoda inflata* cells were significantly smaller in the 28 ℃ treatment (lag, 1.3×10^5 μm^3; log, 7.7×10^4 μm^3; plateau, 3.9×10^4 μm^3, resting cysts, 7.5×10^3 μm^3) than in the 18 ℃ treatment ($P < 0.05$ in all cases; Fig. 2A). Similarly, the small-sized *C. steinii* lost 85% and 69% of its CV during encystment relative to the log phase cells in 18 ℃ and 28 ℃ treatments, respectively. At a given vegetative phase the cell volume was always larger in the cultures reared at 18 ℃ than at 28 ℃ ($P < 0.05$), except for the resting cysts, whose size (about 2.0×10^3 μm^3) was not significantly different between these two temperature treatments (Fig. 2A).

The chilling-induced unstable cysts of both *Colpoda* species were generally larger than the resting cysts, but smaller than the plateau phase cells (Fig. 2A). In the treatment of 18 ℃, the volumes of unstable cysts of *C. steinii* and *C. inflata* were on average 5.3×10^3 and 0.21×10^5 μm^3, respectively (Fig. 1C, 2A). A similar pattern of unstable cyst size was observed for the treatments of 28 ℃ (Fig. 2A). Assuming that the *C. steinii* and *C. inflata* cells were globular in body shape, the equivalent spherical diameter (ESD) of the cells ranged from 13 to 29 μm and from 25 to 74 μm, respectively, with cross-phase patterns similar to these of the cell volume (Fig. 2B).

Macronuclear volume (MV) exhibited a similar trend to the cell volume in both *Colpoda* species, i.e., decreasing gradually through lag, log, and plateau phases to resting cyst, regardless of cultivation temperatures (Fig. 2C). *Colpoda inflata* had consistently a larger MV than *C. steinii* at any specific phase ($P < 0.05$). When the MV was relatively smaller (e.g., MV < 500 μm^3, or macronuclear diameter < 10 μm), the shrink of MV of both species became consistently significant in the 18 ℃ treatments relative to the 28 ℃ treatments. However, when the macronucleus was larger (i.e., macronuclear diameter > 10 μm), the effect of temperature increase on MV was insignificant ($P > 0.05$; Fig. 2C).

The nucleocytoplasmic ratio of two *Colpoda* species ranged from approximately 1% to 8%, and tended to progressively increase from lag, log, to plateau phases and resting cysts (Fig. 2D). The log-phase cells of *C. steinii* had the lowest nucleocytoplasmic ratios (on average 2.92% to 2.61% at 18 ℃ and 28 ℃, respectively), which were about 1.13 to 1.32 times lower than these in lag and plateau phases, respectively. Culturing at the higher temperature generally did not induce significant decreases in the nucleocytoplasmic ratio in most growth phases of either species ($P > 0.05$), except for resting cysts of *C. steinii*, which had a much higher nucleocytoplasmic ratio (on average 7.93%) at 18 ℃ than that at 28 ℃ (3.82%). Compared with the small species, *Colpoda inflata* usually had lower cytoplasmic volume ratios in all phases and at both temperatures (Fig. 2D). Regression analysis showed that macronuclear volume scaled well with $CV^{0.83}$ (Fig. 2E); the nucleocytoplasmic ratio fit well to a power-lower function of $ESD^{-0.522}$ (Fig. 2F):

$$\lg(MV) = 0.83 \lg(CV) - 0.87, \text{ or } MV = 0.136\, CV^{0.83} \quad (1)$$

$$R^2 = 0.90,\ P < 0.001,\ n = 733;$$

$$MV/CV = 0.136\, CV^{-0.17} = 0.151\, ESD^{-0.52} \quad (2)$$

$$CV = 5.14\, ND^{3.63} \quad (3)$$

Where *ND* is the mean macronuclear diameter of *Colpoda* spp.

Variations in single-cell rDNA and rRNA copy numbers and concentrations

The per-cell rDNA and rRNA copy numbers varied significantly among growth phases (ANOVA, $P < 0.001$), showing a consistently decreasing trend from the lag, log, and plateau phases to the resting cyst stage, for both *Colpoda* species and at both temperatures. The resting cysts of both *Colpoda* species lost 50% ~ 90% of rDNA and over 89% ~ 99.99% of rRNA copies relative to the cells in log phase (Fig. 3A, B). In the 18 ℃ treatment, a lag-phase cell of *C. steinii* had on average $(10.2 \pm 1.22) \times 10^3$ rDNA copies. The CN was about 2 and 4.6 times higher than that in the log [$(5.4 \pm 0.7) \times 10^3$ copies] and plateau phases [$(2.2 \pm 0.3) \times 10^3$ copies], respectively. The rDNA amount reduced greatly in the resting cysts of this species, with only about 1000 copies per cyst (Fig. 3A). Although the unstable cysts of *C. steinii* were smaller than the plateau-phase cells, the former had a similar copy number of rDNA [$(2.0 \pm 0.2) \times 10^3$] as the latter. Compared with the lower temperature treatments, *C. steinii* cultured at 28 ℃ had lower per-cell rDNA copy numbers, particularly for the cells at log and plateau phases ($P < 0.05$); however, the number of rDNA copies

in the resting cysts of this species did not change significantly at the warmer condition ($P = 0.69$).

The large-sized *Colpoda* species had many more rDNA copies than the small-sized congener at any life cycle stages (Fig. 3B). A single cell of *C. inflata* reared at 18 ℃ had [4.48×10^4], [1.98×10^4], and [1.33×10^4] rDNA copies at the lag, log, and plateau phases, respectively. Phase-specific comparisons of the cells between these two temperature treatments showed that the effect of warming was not significant for this species ($P > 0.05$). The resting and unstable cysts of *C. inflata* contained about 2500 and 8100 rDNA copies, respectively, which were about 3.3 and 4.2 times than those of *C. steinii* (Fig. 3B).

The cellular rRNA copies were far more abundant, and varied more dramatically across growth stages, than the rDNA copies in both *Colpoda* spp. (Fig. 3A, B). In the 18 ℃ treatments, a single cell of *C. steinii* had about 3.0×10^7, 1.0×10^7, 5.7×10^6, and 3.4×10^4 rRNA copies at the lag, log, plateau and resting cyst stages, respectively (Fig. 3A). At the same temperature, the rRNA molecules were much more abundant in *C. inflata*, with about 1.7×10^8, 1.3×10^8, 3.2×10^7 and 3.1×10^4 across these phases (Fig. 3B). Although smaller than the plateau-phase cells, the unstable cysts had relatively similar (in *C. steinii*) or even higher number of rRNA copies (in *C. inflata*) (Fig. 3A, B). Comparing the two temperature treatments, warming always led to a significant decrease in cellular rRNA amount of both species and at all the vegetative stages plus the unstable cysts ($P < 0.05$). Nevertheless, there were no significant differences in the cellular rRNA abundance in resting cysts at either temperature (Fig. 3A, B). A cell at any vegetative growth phase of these two species had approximately 200 to 5000 times more rRNA copies than resting cysts (Fig. 3A, B).

When per-cell copy numbers of rDNA and rRNA were standardized to cell volume, the concentrations of these two ribotypes remained relatively stable across most growing phases and cystic stages (Fig. 3C). In both temperature treatments, the mean cellular rDNA concentrations ranged mostly between 0.4 and 0.8 copies μm^{-3} in *C. steinii*, and were slightly lower (from 0.2 to 0.3 copies μm^{-3}) in *C. inflata*, showing no significant differences across lag, log, plateau and resting cystic phases in either species ($P > 0.05$). The only exception lied in a significantly lower concentration (0.44 copies μm^{-3}) at the log phase (relative to the lag phase) of *C. steinii* in the warmer treatment (Fig. 3C); and there was a significant difference of concentrations (on average 0.20 vs. 0.35 copies μm^{-3}) in resting cysts of *C. steinii* between two temperature treatments. The culturing temperature prior to chilling affected the rDNA concentrations in subsequently formed

unstable cysts of both species: the cellular rDNA concentrations in the unstable cysts of both species at 28 ℃ were twice these at 18 ℃ (Fig. 3D).

Generally speaking, the rRNA concentration varied within relative larger ranges in the vegetative cells (1000 - 2200 copies μm^{-3} in *C. steinii*, and 560 - 1500 copies μm^{-3} in *C. inflata*), but the difference at a given growth phase was mostly insignificant (Fig. 3C, D). Nevertheless, differing from the rDNA molecules that still sustained reasonably high cellular concentrations during formation of resting cysts via the plateau phase, the rRNA concentrations became significantly lower in resting cysts of both *C. steinii* (27 copies μm^{-3} at 18 ℃, and 380 copies μm^{-3} at 28 ℃; Fig. 3C) and *C. inflata* (0.13 copies μm^{-3} at 18 ℃, and 2.1 copies μm^{-3} at 28 ℃; Fig. 3D). Culturing temperature seemed to not affect rRNA concentrations in the vegetative cells most of the time (Fig. 3C, D). The unstable cysts of *C. steinii* (1120 copies μm^{-3} at 18 ℃, and 1895 copies μm^{-3} at 28 ℃) had similar concentrations of rRNA with the vegetative cells, while *C. inflata* (5336 copies μm^{-3} at 18 ℃, and 3734 copies μm^{-3} at 28 ℃) had many more rRNA molecules than its vegetative forms. Furthermore, rRNA concentrations in unstable cysts were significantly different between these two treatments (Fig. 3C, D).

There were minor differences between two *Colpoda* species in terms of the patterns of rRNA to rDNA CN ratio across growth phases and between two temperature treatments (Fig. 3E, F). The rRNA: rDNA CN ratios in *C. steinii* mostly ranged from 2000 to 4000, without statistical differences among the lag, log, plateau and unstable cystic stages ($P > 0.05$; Fig. 3E). Nevertheless, the rRNA: rDNA ratios in *C. inflata* decreased from 10000 to 2000 when the population growth at 18 ℃ entered into plateau phase; and this species also exhibited a significantly high rRNA: rDNA ratio in unstable cysts induced from the actively growing cells in the 18 ℃ treatment (Fig. 3F). Furthermore, while the rRNA: rDNA ratios in log-phase cells, unstable, and resting cysts of *C. inflata* significantly dropped at the higher culturing temperature (Fig. 3F), the same was not observed in *C. steinii* (Fig. 3E). Nevertheless, a trait shared by both species was that the rRNA: rDNA ratios (150 – 400 in *C. steinii*, and 2 – 16 in *C. inflata*) were much lower in resting cysts than in the cells at all other phases (Fig. 3E, F).

Linking ribotypic with phenotypic traits

Based on all CN data of vegetative and cystic cells of these two *Colpoda* spp., correlation and

linear regression analyses showed that both ribotypic CN traits (rDNA and rRNA copy number per cell, $rDNA_{CNPC}$ and $rRNA_{CNPC}$) were positively and significantly related to CV (P <0.01). Ribotype CNs could well fit to linear regression curves (Fig. 4A):

$$\lg(rDNA_{CNPC}) = 0.76 \lg(CV) + 0.61, \text{ or } rDNA_{CNPC} = 4.07\ CV^{0.76} \quad (4)$$

$R^2 = 0.91$, $P < 0.001$, $n = 20$;

Assuming the cell is globular in shape, with an equivalent spherical diameter *(ESD)*, then:

$$rDNA_{CNPC} = 2.49\ ESD^{2.28} \quad (5)$$

$$\lg(N \cdot rDNA_{CNPC}) = \lg N + 2.28 \lg ESD + 0.396 \quad (6)$$

Where N is the number of cells of identical size; $N \cdot rDNA_{CNPC}$ is the total rDNA copy number of the population that can be experimentally determined (for example, by using qPCR). The scaling relationships and R^2 scores indicated that the $rDNA_{CNPC}$ of these two *Colpoda* species could be accurately predicted using biovolume (equation 4) or *ESD* (equations 5 and 6) of cells, no matter whether the cells were at lag, log, plateau, or in unstable or resting cystic forms. Furthermore, equation (6) clearly indicates that the total rDNA CN of a population is determined not only by cell abundance (N), but also by cell size (*ESD*).

As for rRNA, the correlation between $rRNA_{CNPC}$ and CV across all life cycle phases including resting cysts (+RC) was significant. However, the R^2 score (37%) was only moderate (Fig. 4A):

$$\lg(rRNA_{CNPC}) = 1.24 \lg(CV) + 1.69,\ R^2 = 0.37,\ P = 0.005,\ n = 20 \quad (7)$$

Apparently, the rRNA amount in resting cysts of *Colpoda* species was extremely lower and not easily predicted when using cell size. Nevertheless, when the rRNA CN data of the resting cysts (i.e., the four blue full diamonds that are discrete from other points in Fig. 4A) were excluded from the analysis (-RC), we obtained:

$$\lg(rRNA_{CNPC}) = 0.87 \lg(CV) + 3.67, \text{ or } rRNA_{CNPC} = 4677\ CV^{0.87} \quad (8)$$

$R^2 = 0.84$, $P < 0.001$, $n = 16$;

$$rRNA_{CNPC} = 2664\ ESD^{2.61} \quad (9)$$

$$\lg(N \cdot rRNA_{CNPC}) = \lg N + 2.61 \lg ESD + 3.43 \quad (10)$$

By removing resting cystic data, the re-modeled rRNA CN and cell size relationship became much more robust ($R^2 = 0.84$). Therefore, based on a combination of equations (6) and (10), which do not take resting cysts into account, we have:

$$\lg(N \cdot rRNA_{CNPC}) - \lg(N \cdot rDNA_{CNPC}) = 0.33 \lg ESD + 3.034$$

Or, $\lg(rRNA_{CNPC} / rDNA_{CNPC}) = 0.33 \lg ESD + 3.034$ (11)

Equation (11) indicates that, given that all cells in a population are non-resting cysts, the rRNA: rDNA copy number ratio depends on a single factor, *ESD* or cell size.

Since the total rDNA pool ($rRNA_{total} = N \cdot rRNA_{CNPC}$) and the total rDNA pool ($rDNA_{total} = N \cdot rDNA_{CNPC}$) can be experimentally quantified (e.g., qPCR), then:

$\lg[(rRNA_{total} - rRNA_{rc}) / (rDNA_{total} - rDNA_{rc})] = 0.33 \lg ESD + 3.034$, (12)

Where $rRNA_{rc}$ and $rDNA_{rc}$ are the total cellular rRNA and rDNA CNs in the resting cysts existing in the population. Assuming that the proportion of resting cysts in the rDNA pool is *cyst*%, and their fraction in the rRNA pool is negligible (about 0.02% to 0.5% relative to a vegetative cell of *Colpoda* spp.), then:

$\lg[(rRNA_{total})/(rDNA_{total} - rDNA_{total} \cdot cyst\%)] = 0.33 \lg ESD + 3.034$ (13)

Thus, the rDNA proportion of non-resting cells (*NRC*%) in a population can be estimated as follows:

$NRC\% = 1 - cyst\% = (rRNA_{total}/rDNA_{total}) / (1081 \cdot ESD^{0.33})$ (14)

The correlations between *MV* of cells at all life cycle stages and ribotype CNs exhibited patterns similar to the observed for CV (Fig. 4B):

$\lg(rDNA_{CNPC}) = 0.90 \lg(MV) + 1.44$ or $rDNA_{CNPC} = 27.54\ MV^{0.9}$ (15)

$R^2 = 0.93$, $P < 0.001$, $n = 16$;

$\lg(rRNA_{CNPC}) = 1.70 \lg(MV) + 2.28$ or $rRNA_{CNPC} = 190.55\ MV^{1.7}$ (16)

$R^2 = 0.50$, $P = 0.002$, $n = 16$;

The rRNA CN data did not fit the model very well. However, when the rRNA data of resting cysts were not considered, the explanation of variance in rRNA CNPC could be greatly improved:

$\lg(rRNA_{CNPC}) = 1.05 \lg(MV) + 4.47$ or $rRNA_{CNPC} = 29512\ MV^{1.05}$ (17)

$R^2 = 0.83$, $P < 0.001$, $n = 12$.

According to Fu and Gong (2017), the per-cell rRNA CNs in the log phase cells of *E. vannus* and *S. sulcatum* were at similar levels as these in *Colpoda* cells of similar cell sizes [the lg(*CV*) ranging from 3.3 to 4.1; Fig. 4C]. However, these two marine species had about 30 ~ 80 times more rDNA copies (109,000 ~ 263,000 per cell) than the *C. steinii* cells (1300 ~ 9540 copies per cell)

within the same cell size range (Fig. 4C). In other words, the previous data of *E. vannus* and *S. sulcatum* data largely followed the scaling relationship between rRNA and CV of non-resting *Colpoda* (R^2 = 0.86, P < 0.001), but was not consistent with the rDNA-CV relationship described in the present study (R^2 = 0.05, P < 0.001).

Interestingly, based on a combination of datasets comprising both these previously reported for *Euplotes vannus* and *Strombidium sulcatum* (n = 8; Fu and Gong, 2017) and the present data for *Colpoda* spp. (n = 4), the maximum growth rate (r) of these species at a given culturing temperature (t) can be well predicted by $rDNA_{CNPC}$, but not $rRNA_{CNPC}$ (n = 12), as follows:

$$\ln r = 0.051\, t - 0.474 \ln (rDNA_{CNPC}) + 4.192 \quad (18)$$

R^2 = 0.911, adjusted R^2 = 0.891, P < 0.001, n = 12 (Fig. 4D)

$$\ln r = 0.131\, t + 0.229 \ln (rRNA_{CNPC}) - 6.323 \quad (19)$$

R^2 = 0.457, adjusted R^2 = 0.336, P = 0.064, n = 12

$$\ln r = 0.084\, t + 0.289 \ln (rRNA_{CNPC} : rDNA_{CNPC}) - 3.121 \quad (20)$$

R^2 = 0.799, adjusted R^2 = 0.755, P < 0.001, n = 12

These predictions of maximum growth rate based on $rDNA_{CNPC}$ or $rRNA_{CNPC}$: $rDNA_{CNPC}$ outperformed the ones based on CV:

$$\ln r = 0.126\, t + 0.206 \ln (CV) - 4.420 \quad (21)$$

R^2 = 0.45, adjusted R^2 = 0.33, P = 0.069

Dominance of a single haplotype in single-cell rDNA and rRNA pools

A total of 124 rDNA and cDNA samples derived from 124 single cells of the four ciliate species were successfully sequenced. After quality filtering, removal of chimeric and singleton sequences, the cleaned reads of 18S rDNA or cDNA fragments were subjected to statistical analyses to characterize the distributional patterns of dominant haplotypes or variants under different conditions (Table S1). In each species, there was a single haplotype, which was numerically dominant (referred to as dominant haplotype, DH), and many variants in the rDNA (or rRNA) pool (Table S1).

The variant sequences differed from the DH by having many single nucleotide substitutions. The relative abundance of the DH in a single cell varied widely, depending on species, rDNA or rRNA pools, life cycle stage, and temperature (Fig. 5A - D). The DHs accounted for 68% - 86% in

Colpoda spp., the proportion of which was higher than that of *E. vannus* and *S. sulcatum* (37% to 46%). The DH percentages in the rDNA pools appeared to be higher than in the rRNA pools in both *Colpoda* species (*C. steinii:* 84.44% ±0.52% vs. 79.92% ±0.80%; $P < 0.001$, $n = 20$; and *C. inflata*: 82.55% ± 1.13% vs. 74.97% ± 2.10%; $P = 0.006$, $n = 20$). At a given life cycle stage and temperature ($n = 3$), however, the differences in DH percentage between rDNA and rRNA pools were frequently not significant with some exceptions. The DH had much lower proportions in the rRNA pools ($P < 0.05$) in the 28 ℃ treatments of resting cysts of *C. steinii* (Fig. 5A), and all the treatments of *C. inflata* (Fig. 5A, B), while DH proportion was higher ($P < 0.05$) in the rDNA pools than in the touchdown treatments (16*) of *E. vannus* (Fig. 5C).

The resting cysts of *Colpoda* spp. were frequently comparable to the log-phase cells in terms of DH proportions in both rDNA and rRNA pools (Fig. 5A, B). Nevertheless, significant differences in DH proportions between these two life cycle stages were found for *C. inflata* reared at 28 ℃, in which the resting cysts had lower levels in both rDNA (81.70% vs. 85.02%) and rRNA pools (78.85% vs. 82.73%) (Fig. 5B).

The effect of temperature on DH proportion was significant in several pairwise comparisons (Fig. 5B, C). Compared with the treatments of 18 ℃, the DH proportion in the rDNA pool significantly decreased ($P < 0.05$), but the opposite was observed in the rRNA pool of resting cysts of *C. inflata* ($P < 0.05$; Fig. 5B). In the actively growing cells of *E. vannus*, the lowest DH proportion in rRNA pool was found in the treatments of 21 ℃. This pattern, however, was not observed for the DH in the rDNA pool of this species (Fig. 5C).

Single-cell landscape of rDNA and rRNA variants

Despite many more quality reads having been obtained, fewer rDNA variants were detected in single cells of *C. steinii* (300 ~ 700 cell^{-1}) and *C. inflata* (400 ~ 800 cell^{-1}), compared with those in *E. vannus* (3200 ~ 3400 cell^{-1}) and *S. sulcatum* (2200 ~ 2700 cell^{-1}) (Fig. 5E; Table S1). In contrast, the single-cell rRNA pools of *C. steinii* (600 ~ 900 cell^{-1}), *C. inflata* (850 ~ 950 cell^{-1}), *E. vannus* (3000 ~ 3600 cell^{-1}) and *S. sulcatum* (2100 ~ 3000 cell^{-1}) generally exhibited higher numbers than their rDNA variants (Fig. 5F; Table S1). Regression analysis indicated that the number of rDNA variants was positively related with rDNA CN per cell ($R^2 = 0.97$, $P < 0.001$; Fig. 5E), whereas the number of rRNA variants in a single cell was not significantly related to cellular rRNA CN of these

species (R^2 = 0.093, P > 0.21; Fig. 5F). These patterns remained even when the variants were called by randomly sampling an equal number (1600) of rDNA and rRNA reads per sample (Table S1).

The hypotheses that life cycle stage and temperature affect the numbers of rDNA and rRNA variants were also tested (Fig. 6A). To standardize and minimize the uneven number of reads obtained from each sample, the variants were called by randomly sampling an equal number (1600) of rDNA or rRNA reads per sample (Table S1). Significant differences in numbers of rDNA and rRNA variants were exclusively found among certain treatments of the *Colpoda* species, but never among the temperature treatments of log-phase *E. vannus* and *S. sulcatum*. More specifically, contrasting numbers of rRNA variants (4 out of 6 cases) occurred more often than those of rDNA variants (2 out of 6 cases). For example, at 18 ℃, a resting cyst of both *C. steinii* (118 ± 6) and *C. inflata* (116 ± 2) was significantly richer in rRNA variants than a log-phase cell of these species (102 ± 2 and 103 ± 4, respectively; P < 0.05). The cell phase effect on rDNA variant numbers was significant only in the treatments of *C. inflata* reared at 28 ℃ (P < 0.05). The number of rDNA (and rRNA) variants differed between the two temperature treatments (P < 0.05) in resting cysts of *C. inflata*; whereas a temperature effect on the number of ribotype variants in log cells was detected only in *C. steinii* (Fig. 6A).

By rarefying at 1600 reads and clustering operational taxonomic units (OTUs) at thresholds ranging from 90% to 99%, we identified the maximum differences among the rDNA and rRNA variants in single cells of these ciliate species (Fig. 6B). The highest divergence of both rDNA and rRNA variants was 9%, which was observed in *C. steinii*. The lowest divergence was observed in *S. sulcatum*, in which intra-individual differences of rDNA and rRNA variants did not exceed 1%. Both *C. inflata* and *E. vannus* exhibited intermediate levels of divergence in both rDNA (6% and 7%) and rRNA (8% and 4%) (Fig. 6B).

The obtained numbers of OTUs ranged from 1 to 5 at a cutoff of 99%, and gradually decreased with lower cutoffs. Typically, at the 97% cutoff that has been popularly used for metabarcoding surveys, on average of 1 to 2 OTUs remained for the *Colpoda* species. The resting cysts usually appeared to have more OTUs than the log-phase cells, however, this was significant (P < 0.05) only in 3 out of 8 pairwise comparisons for *Colpoda* spp. The temperature effect on OTU numbers in single cells was even less frequent, observed only in 1 out of 8 comparisons for *Colpoda*, and in none for *E. vannus* and *S. sulcatum* (P > 0.05) (Fig. 6B).

Nucleotide polymorphisms

The intra-individual sequence variations of rDNA and rRNA variants in the single cells of the four ciliate species were exclusively single nucleotide polymorphisms (SNPs). By setting the consensus sequence (the DH) as the reference, the number of polymorphic sites and types of nucleotide substitutions were identified (Figs 7 and 8). The frequency of polymorphic sites (SNP density) ranged from 4.0×10^{-4} to 2.9×10^{-3} in rDNA, and from 4.9×10^{-4} to 6.3×10^{-3} in rRNA. Nucleotide replacements occurred in all positions along the sequenced rDNA and rRNA fragments, most of which had a frequency lower than 3.0×10^{-3}. Fifteen sites were highly polymorphic (with a replacement frequency of $> 3.0 \times 10^{-3}$), and their positions were conserved in the two *Colpoda* species and in both ribotypes. Likewise, 20 positions exhibited high nucleotide replacement frequencies in both rDNA and rRNA in *E. vannus* and *S. sulcatum* (Fig. 7A). Relative to the log phase cells of *Colpoda*, the resting cysts often had significantly higher frequencies of nucleotide substitutions (SNP density) in rRNA, but not rDNA. The effect of temperature was only significant for *E. vannus*, in which the SNP density of rDNA was much higher in the touchdown (16* ℃) than in the treatment at 16 ℃, and even higher at 21 ℃ than all other treatments of this species (Fig. 7B).

Overall, the transition: transversion (Ts: Tv) ratio in rDNA and rRNA was conserved within species, but varied from 1.1 to 3.0 among the four ciliate species (Fig. 8). Temperature and encystment had no significant effects on the Ts: Tv ratio within a species either ($P > 0.05$). However, individual nucleotide substitution categories showed different patterns. For example, transitional A/G substitutions were more frequent than C/T substitutions in both rDNA and rRNA transcripts of all ciliate species, except for *C. steinii*, which showed the opposite pattern, especially between two life cycle stages. In the 18 ℃ treatments of *C. steinii*, the frequency of A/G substitutions in rDNA was significantly lower in resting cysts (on average 10.3%) than in log-phase cells (22.4%), whereas the reverse was observed for transitional C/G substitutions (43.4% for resting cysts and 29.6% for log-phase cells). Transversions in the rDNA and in the expressed transcripts appeared to be frequently higher in log phase cells vs. resting cysts of *Colpoda* spp. in both temperature treatments ($P < 0.05$). In the rDNA of *C. inflata*, G/C substitutions occurred more frequently in resting cysts (on average 5.0%) than in log cells (3.5%) at 28 ℃. In contrast, in rRNA transcripts of *C. inflata*, the cell phase-wise differences were observed in 5 of the 6 nucleotide substitution

categories, especially in the 28 ℃ treatments (Fig. 8).

There were only a few cases in which the frequency of nucleotide substitution was significantly different between temperature treatments (Fig. 8). Higher frequencies in transversional G/T (17.8% vs. 13.6% in *C. steinii*) and G/C substitutions (5.0% vs. 2.9% in *C. inflata*) occurred in resting cysts at 28 ℃ (vs. at 18 ℃). Nevertheless, the variants with G/T substitutions in log-phase cells of *C. steinii* were more highly expressed at the lower temperatures (17.1% vs. 15.2%).

DISCUSSION

Allometric scaling relationship of nuclear volume to cell volume in *Colpoda*

Single cells of two *Colpoda* species in all growing phases and cystic forms obtained from two temperature treatments were fixed, stained with protargol and their cell and nuclear volumes measured. Both volumes progressively reduced from lag, log, and plateau phases to resting cysts, the latter being a phenotypic trait common in many protists (e.g., a scuticociliate, Pérez-uz and Guinea, 2001; a dinoflagellate, Anderson and Lindquist, 1985). In parallel, the N/C ratio in both *Colpoda* species significantly increased, especially after resting cyst formation. The increase was about a 3-fold difference in *C. steinii* reaching an N/C ratio of 7.31% and in *C. inflata* 4.35% (Fig. 2D, F). These findings are in contrast to the "karyoplasmic" ratio theory, which postulates that eukaryotic cells of the same type or species maintain a constant N/C ratio. For example, despite fission and budding yeasts spanning a large range of cell sizes (10 ~ 300 μm^3), their N/C ratio is approximately 7% to 8% (Jorgensen et al., 2007; Neumann and Nurse, 2007). Our data indicate that the N/C volume ratio of the two *Colpoda* species examined herein inversely scales with cell volume to a power of -0.174. Thus, both species display allometry similar to that previously described for amoebae (Rogerson et al., 1994) and *Xenopus* cells during early embryonic development (Jevtić and Levy, 2015), rather than isometry of N/C ratio with CV, which has been commonly observed in many other eukaryotes (Reber and Goehring, 2015). In this study, the *Colpoda* cells covered a broad size range (from 7500 μm^3 to 2.14×10^5 μm^3) at all life cycle stages allowing for a good fit of the scaling relationship with power-law functions. Linear models might fit the data equally well (so that missed the curved trajectory corresponding to a large size range) with relatively narrow ranges of cell size or very large cells. According to the ciliate-based equation 2, calculations based on the average CV of wild-type fission and budding yeasts yield the same N/C ratios as experimentally

determined, indicating that the allometry between N/C ratio and CV could be widely applicable within and among eukaryotic species. Given that it is relatively easy to measure the volume of nucleus, which is usually globular or ellipsoid in living and/or fixed materials, the N/C ratio allometry provides a tool to calculate biovolume (biomass) of amorphous cells (e.g., amoebae) using nuclear size (Rogerson et al., 1994).

Ribotype copy number variations across different phases of growth and cystic forms

Due to macronuclear polyploidy and micronuclear diploidy in ciliates, most rDNA copies quantified and sequenced in this study were of macronuclear origin. Substantial variations in rDNA and/or rRNA quantities have been previously recorded in randomly selected individuals of ciliates (Gong et al., 2013; Wang et al., 2019), log phase populations (Fu and Gong, 2017), and among cells of different phases of growth or physiological states in a range of protistan species (e.g., a *Tetrahymena* ciliate, Engberg and Pearlman, 1972; a raphidophyte, Main et al., 2014; a foraminifer strain, Parfrey et al., 2012; and dinoflagellates, Galluzzi et al., 2010; Eckford-Soper and Daugbjerg, 2016; Nishimura et al., 2016). Nevertheless, our study provides the first evidence of linkage between ribotypes and phenotypes across life cycle stages of protists. Specifically, several ribotypic traits (i.e., the per-cell CN, cellular concentrations of rRNA and rDNA molecules, along with their CN ratio) are quantitatively linked with cell and macronuclear size, across all growing phases and dormant cystic forms. This finding extends our understanding obtained by observations of log phase cells of *E. vannus* and *S. sulcatum*, and reinforces previous recommendations, that in molecular protistan ecology, ribotype CNs have to be interpreted to reflect biomass rather than solely cell abundance (Fu and Gong, 2017).

Chilling of actively growing *Colpoda* cells at 0 ~ 4℃ for a few hours artificially induced formation of unstable cysts (Fig. S1), an event that was accompanied by significant reduction in per-cell rDNA and rRNA CNs, as well as, cell size (Fig. 2A; 3A, B). Freezing raw environmental samples (e.g. raw soil, sediment or water samples) temporarily to preserve microbiomes is commonly used in molecular ecology. Herein, we show that this practice might artificially alter both phenotypic and ribotypic traits of certain protistan populations and thus the whole community structure. This could lead to underestimation of their biomass and proportions of rDNA and rRNA quantities in the ribotypic pools. Nevertheless, chilling treatment is a simple, non-destructive

approach that arrests growing cells at the unstable cyst stage, thus narrowing down the cell size spectrum of a population consisting of different-sized cells in various growth phases, while preserving cell numbers in the original samples. Thus, chilling treatment has the potential to enhance the accuracy in estimating population abundances using rDNA-based qPCR or hybridization methods. Abundance estimates derived from either method tend to be inconsistent due to variable rRNA gene content across growth phases in natural populations of harmful marine microalgae (Galluzzi et al., 2010; Main et al., 2014; Eckford-Soper and Daugbjerg, 2016; Nishimura et al., 2016). Second, we provide evidence that both types of *Colpoda* cysts follow the rDNA CN-CV relationship (Fig. 4; Equations 4 and 5), so their biomass can be reasonably predicted in rDNA-based molecular surveys. Third, the two types of cysts have variable amount of rRNA or ribosomes. In the unstable cysts, the amount of rRNA copies corresponds well with cell size, whereas a resting cyst has much fewer rRNA molecules. This is a unique ribotypic trait of resting cysts that cannot readily be explained by their small cell size (Fig. 4). These results clarify the ribotypic distinctness between unstable and resting cysts. Herein, we demonstrate a theoretical framework that makes use of the experimentally determined rRNA:rRNA ratio of a given *Colpoda* species. The framework can be adopted to estimate the proportion of resting cysts in the rDNA pool of a population. Importantly, our proposed framework takes into account cell size (see Equation 14), indicating that it affects estimation of resting cysts. This implies that caution should be taken in using rRNA: rDNA ratios to compare within and between species/groups of contrasting cell sizes. Thus, qPCR could be applied in future studies for quantifying cysts of *Colpoda*, and/or probably also other protists, in environmental samples.

Cellular rRNA content scales inversely with cell size, but maximum growth rate depends on rDNA content

Previously, a scaling relationship between rRNA content and cell size of log-phase cells of two protist species and five species of bacteria and archaea was proposed (Fu and Gong, 2017). This study provides evidence that the scaling relationship generally holds, irrespective of life cycle stages. These findings collectively support the universality of the scaling law between rRNA content and cell/body size applying to micro- to macro-organisms (Gillooly et al., 2005). Nevertheless, the scaling relationship did not apply to resting cysts, as they exhibited significantly

lower rRNA than expected, indicating that rRNA is a suitable molecular marker for not only revealing "active" components, but also for providing a biomass-based view of community structure of microbial communities. Previous studies of mock protistan communities showed consistent patterns using rRNA and cell counting approaches (Weber and Pawlowski, 2013).

Unlike rRNA, the scaling relationship between rDNA and cell volume was not uniform for any of the four ciliate species examined. Instead, two separate functions were applied; one for *Euplotes* and *Strombidium* (rDNA ~ $CV^{0.44}$; Fu and Gong, 2017) and another for *Colpoda* spp. (rDNA ~ $CV^{0.76}$; this study). This is primarily due to the much higher cellular rDNA content in *E. vannus* and *S. sulcatum* (23 - 59 copies per μm^3) than in the similar sized cells of *Colpoda steinii* and *C. inflata* (0.2 - 0.8 copies per μm^3) (Fig. 4C). The disproportion between per-cell rDNA copy number and cell size was also pointed out by Wang et al. (2019). The variable rDNA content between Spirotrichea and Colpodea may stem from their genomic distinctness. Spirotrichean ciliates are well known for their highly polyploidized genomic macronuclear DNA (Prescott, 1994). The higher rDNA content also implies higher genomic DNA content and larger macronuclear volumes (Cavalier-Smith, 1978). In support of this, both *E. vannus* and *S. sulcatum* have disproportionately large macronuclei (N/C ratios about 4.71% and 2.73%, respectively) that do not correspond to the predicted values (1.57% and 2.43%) of the *Colpoda*-based model (Equations 1 and 2) and their actual average cell volumes (2.34×10^5 and 1.93×10^4 μm^3). This indicates that larger macronuclear size does contribute to high rDNA content in these two spirotricheans. Even if the "enlarged" macronuclear sizes of *E. vannus* and *S. sulcatum* are taken into consideration, their calculated per-cell rDNA copy numbers according to the *Colpoda*-based function (Equation 15), will be only about 1/2 and 1/16 of these experimentally determined. This suggests that the high rDNA content of spirotricheans is not just due to their unusual phenotype (enlarged macronuclei), but that certain, as yet undiscovered, mechanisms for genomic innovation may also be at play.

Interestingly, *Colpoda steinii* grew 7 to 12 times faster than *E. vannus* and *S. sulcatum*, despite these three species having comparable cell size and cellular rRNA content. The model parameterized with rDNA performed much better than the one with rRNA in predicting growth rate (Equations 18 and 19). This indicates that, besides temperature (which modulates cell size via the temperature-size rule), cellular rDNA content is an important factor in determining generation time of these protists. This observation seems to violate the grow rate hypothesis (GRH) that has been

repeatedly validated in diverse organisms, which postulates that a high growth rate depends on a high rRNA or ribosomal concentration, or phosphorus (P) content in biomass (Elser et al., 2000). To reconcile the two, we propose that growth rate is determined by rRNA content, but can be modified by rDNA contents. In other words, growth rate depends mainly on rDNA, when the cells have similar cell sizes or rRNA contents (see Fig. 4C).

Existing studies on genomic content and growth rates of various organisms can shed light in understanding the mechanisms underlying modulation of cell growth rate by rDNA content. For instance, in a previous study, haploid cells of budding yeast with a smaller cell size grew more rapidly than their diploid counterparts of larger cell size. The observed fitness difference was attributed to their cell surface to volume ratio. Specifically, growth rate was dependent on the transfer of products into cytoplasm generated upon hydrolysis of organic phosphorous by a cell surface-bearing acid phosphatase (Weiss et al., 1975; Mable and Otto, 2001). The surface-to-volume-ratio theory does not seem to apply to phagotrophic ciliates, which graze on food particles through their cytostome and digest them inside cytoplasmic food vacuoles. Nevertheless, the lower nuclear to cell volume ratio of *C. steinii* may provide a relatively larger cytoplasmic space to accommodate food vacuoles, enabling digestion of more bacterial prey and maintenance of a higher rate of material supply for growth than *E. vannus* and *S. sulcatum*. Spirotricheans have a high content of rDNA and genomic DNA, both of which are particularly P- and N-rich. Thus, these ciliates need more element-bearing resources and invest a longer time for DNA replication, synthesis of associated proteins, and cell division (Hessen et al. 2010). Conversely, the similarly sized colpodean ciliate *C. steinii* with fewer rDNA copies and a more streamlined genome could be able to save more P and N to synthesize rRNA and assemble ribosomes for rapid growth.

Intra-individual rDNA and rRNA sequence variations across life cycle stages and at different temperatures

In the present study, the intragenomic polymorphisms of 18S rDNA were examined and a level of divergence of up to 9% was noted. This is comparable to the divergence uncovered using high throughput sequencing in other surveys (13% in radiolarians, Decelle et al., 2014; up to about 16% in a *Protocruzia* ciliate, Zhao et al., 2019). Previous studies of rDNA polymorphism using clone libraries and Sanger sequencing yielded lower intragenomic divergence (< 2%) in ciliates (Gong et al.

2013; Wang et al., 2017; Wang et al., 2019) and diatom species (0.57%-1.81%, Alverson and Kolnick, 2005), while divergence was moderate (about 5%) in foraminifera (Weber and Pawlowski, 2014). These results suggest that estimation of intra-individual variability in rDNA sequences depends on sequencing depth, and that variability is likely much higher than previously recognized for many protistan groups. Use of polymerases of varying fidelity also affects polymorphism estimations (Wang et al., 2017). Intragenomic polymorphisms in rDNA along with experimental bias could inflate species richness estimations (Gong et al., 2013; Caron and Hu, 2019). Fortunately, the observed variation seemed to have negligible effect on the rDNA-based OTU number of a protistan species, at least under the conditions examined in this study (temperature gradients; and cystic vs. rapidly growing life cycle stages), provided that the OTUs were defined at a proper sequence similarity threshold (e.g., 97%; Fig. 6). These results indicate that, even though the OTU richness tends to be inevitably higher than the species richness in a multi-species community, the variation pattern in rDNA-based OTU richness is, to some extent, still informative to reflect organizational changes among a series of communities collected across time and space.

Although intra-individual rDNA polymorphisms have been previously recognized, our study is the first to provide evidence that multiple rDNA variants are extensively expressed in protists, resulting in hundreds to several thousands of rRNA variants (Fig. 6E, F). The variants could combine with ribosomal proteins, giving rise to extremely high ribosomal heterogeneity in these ciliates. Such a high diversity of ribosomes in single-celled eukaryotes is surprising, because ribosomes have long been thought of as homogeneous cellular machinery. A notable exception is the parasitic protist, *Plasmodium berghei*, in which two structurally distinct 18S rRNA transcripts were found (Gunderson et al., 1987). Recent studies have suggested that ribosomal variants could preferentially bind different mRNAs to regulate gene expression and corresponding phenotypes of bacteria under stress conditions (Genuth and Barna, 2018; Kurylo et al., 2018; Song et al., 2019). Given the high intracellular rDNA diversity in diverse protistan groups, the significance of ribosomal heterogeneity in the context of physiological and ecological adaptations of protists inhabiting various ecosystems would be an interesting topic to explore.

The lower Variants% in both rDNA and rRNA pools of the soil species *Colpoda* could be related to their lower ribotypic copy numbers than these of the marine species *Euplotes* and *Strombidium* (Fig. 5E). Analogous to the evolutionary significance of polyploidy (Van de Peer et al.,

2017), it is possible that many of the ribotypic sequences are redundant in single cells of *Euplotes* and *Strombidium*, allowing for increased mutational robustness. This would enhance cellular ribosome heterogeneity thus facilitating adaptation to rapidly changing littoral environments. Interestingly, the number of rRNA variants remained stable when comparing the log and resting cystic stages of *Colpoda* species (Fig. 5E), indicating that shrinkage of the cellular rRNA pool in resting cysts is mainly due to the dominant haplotype being expressed less (Fig. 5A, B), rather than the variants. Keeping a large number of rRNA variants (and by extension, a high diversity of ribosomes) in the resting cysts may be ecologically significant for soil ciliates in maintaining a high metabolic potential to readily respond to favorable environmental conditions.

Previous characterization using clone libraries and Sanger sequencing, detected limited numbers of polymorphic sites, resulting in random distributions of SNPs in rDNA and rRNA variants (Alverson and Kolnick, 2005; Gong et al., 2013; Weber and Pawlowski, 2014). In this study, undersampling was largely overcome by using high throughput sequencing, thus additional attributes of SNPs in rDNA and rRNA fragments could be assessed: (1) within a species, the distributional patterns of polymorphic sites in rDNA and their transcripts were almost identical between rDNA and rRNA; (2) the positions of highly polymorphic sites were conserved between *C. steinii* and *C. inflata*, and between *E. vannus* and *S. sulcatum*; and (3) both rDNA and rRNA had hotspot regions, which exhibited much higher substitution frequencies than other regions (Fig. 7A). Furthermore, the rDNA sequences of all four ciliate species exhibited a higher number of transitions than transversions. This finding is consistent with previous clone-library-based results for four other ciliates (Gong et al., 2013), six diatom strains (Alverson and Kolnick, 2005) and the model plant *Arabidopsis thaliana* (Mentewab et al., 2011), and generally comparable with protein-coding sequences of many other species (Stoltzfus and Norris, 2015). Whole genome mutation accumulation rates of the four ciliate species in this study are not available yet. Nevertheless, compared with previously estimated genomic transition: transversion (Ts: Tv) ratios in *Paramecium biaurelia* (1.90) and *P. sexaurelia* (1.67) (Long et al., 2018), the Ts: Tv ratios of 18S rDNA fragments were slightly lower in *C. steinii* (1.1~1.2) and *C. inflata* (1.3 ~ 1.6), but higher in *E. vannus* (2.8~ 3.0) and *S. sulcatum* (2.1 ~ 2.6) (Fig. 7B). All these new findings are in support of the observed nucleotide replacements in the ribotype variants not being random and likely reflecting the non-concerted evolution nature of rDNA in protists and many eukaryotic organisms.

To the best of our knowledge, this is the first study investigating nucleotide substitution patterns of rDNA and rRNA at different life cycle stages and temperatures. Contrasting frequencies of certain nucleotide substitution categories were exclusively detected between resting cysts and log-phase cells of *Colpoda* species (Fig. 8). This could be a consequence of losing variant copies during the biological process of encystment, during which dramatic changes in nucleolar morphology occur and a large portion of macronuclear chromatin is degenerated via cell autophagy (Gutiérrez et al., 1998). Resting cysts have specialized mRNA and proteins, which have been previously been associated with loss of RNA synthetic capability (Benítez and Gutiérrez, 1997; Gutiérrez et al., 1998). Notably, *C. inflata* undergoes demethylation of macronuclear DNA during encystment (Palacios et al., 1994). Nevertheless, the link between changes in nucleotide polymorphisms and rRNA-derived ribosomal heterogeneity remains unknown. Further investigations are needed to explore the mechanistic links between DNA methylation, rRNA-derived ribosomal heterogeneity, and mRNA translation towards a better understanding of the biology and ecology of protistan adaptations.

Acknowledgments

This work was supported by the grants from the Natural Science Foundation of China (Nos. 31572255 and 41976128), the Marine S & T Fund of Shandong Province for Pilot National Laboratory for Marine Science and Technology (Qingdao) (No. 2018SDKJ0406-4), and the Key Research Program of Frontier Sciences (QYZDB-SSW-DQC013). Thanks are due to Prof. Hongan Long (OUC) for suggestions on discussing nucleotide mutations.

REFERENCES

1. Caron DA, Countway PD, Savai P, Gast RJ, Schnetzer A, Moorthi SD, Dennett MR, Moran DM, Jones AC. 2009. Defining DNA-based operational taxonomic units for microbial-eukaryote ecology. Appl Environ Microbiol 75:5797-5808. https://doi.org/10.1128/aem.00298-09.
2. Corliss JO. Protozoan cysts and spores[M]. eLS, 2001.
3. Padilla DK, Savedo MM. A systematic review of phenotypic plasticity in marine invertebrate and plant systems[M]. In: Lesser M, editor. Adv Mar Biol. 65. Academic Press, 2013, pp. 67-94.
4. Mulot M, Marcisz K, Grandgirard L, Lara E, Kosakyan A, Robroek BJM, Lamentowicz M, Payne RJ, Mitchell EAD. 2017. Genetic determinism vs. phenotypic plasticity in protist morphology. J Eukaryot Microbiol 64:729-739. https://doi.org/10.1111/jeu.12406.
5. McQuoid MR, Hobson LA. 1996. Diatom resting stages. J Phycol 32:889-902. https://doi.org/10.1111/j.0022-3646.1996.00889.x.
6. Persson A. 2001. Proliferation of cryptic protists and germination of resting stages from untreated sediment samples with emphasis on dinoflagellates. Ophelia 55:151-166. https://doi.org/10.1080/00785326.2001.10409482.
7. Ross BJ, Hallock P. 2016. Dormancy in the foraminifera: A review. J Foraminifer Res 46:358-368. https://doi.org/10.2113/gsjfr.46.4.358.
8. Corliss JO, Esser SC. 1974. Comments on the role of the cyst in the life cycle and survival of free-living protozoa. Trans Am Microsc Soc 93:578-593. https://doi.org/10.2307/3225158.
9. Fistarol GO, Legrand C, Rengefors K, Granéli E. 2004. Temporary cyst formation in phytoplankton: A response to allelopathic competitors? Environ Microbiol 6:791-798. https://doi.org/10.1111/j.1462-2920.2004.00609.x.
10. Anderson DM, Rengefors K. 2006. Community assembly and seasonal succession of marine dinoflagellates in a temperate estuary: The importance of life cycle events. Limnol Oceanogr 51:860-873. https://doi.org/10.4319/lo.2006.51.2.0860.
11. Fu R, Gong J. 2017. Single cell analysis linking ribosomal (r)DNA and rRNA copy numbers to cell size and growth rate provides insights into molecular protistan ecology. J Eukaryot

Microbiol 64:885-896. https://doi.org/10.1111/jeu.12425.

12. Erdner DL, Percy L, Keafer B, Lewis J, Anderson DM. 2010. A quantitative real-time PCR assay for the identification and enumeration of *Alexandrium* cysts in marine sediments. Deep Sea Res Part II Top Stud Oceanogr 57:279-287. https://doi.org/10.1016/j.dsr2.2009.09.006.

13. Rivière D, Szczebara FM, Berjeaud J-M, Frère J, Héchard Y. 2006. Development of a real-time PCR assay for quantification of *Acanthamoeba* trophozoites and cysts. J Microbiol Methods 64:78-83. https://doi.org/10.1016/j.mimet.2005.04.008.

14. Gutiérrez JC, Martin-González A, Callejas S. 1998. Nuclear changes, macronuclear chromatin reorganization and DNA modifications during ciliate encystment. Eur J Protistol 34:97-103. https://doi.org/10.1016/S0932-4739(98)80018-7.

15. Parfrey LW, Grant J, Katz LA. 2012. Ribosomal DNA is differentially amplified across life-cycle stages in the foraminifer *Allogromia Laticollaris* strain CSH. J Foraminifer Res 42:151-155. https://doi.org/10.2113/gsjfr.42.2.151.

16. Pillet L, Fontaine D, Pawlowski J. 2012. Intra-genomic ribosomal RNA polymorphism and morphological variation in *Elphidium macellum* suggests inter-specific hybridization in foraminifera. PloS One 7:e32373. https://doi.org/10.1371/journal.pone.0032373.

17. Gong J, Dong J, Liu X, Massana R. 2013. Extremely high copy numbers and polymorphisms of the rDNA operon estimated from single cell analysis of oligotrich and peritrich ciliates. Protist 164:369-379. https://doi.org/10.1016/j.protis.2012.11.006.

18. Decelle J, Romac S, Sasaki E, Not F, Mahé F. 2014. Intracellular diversity of the V4 and V9 regions of the 18S rRNA in marine protists (Radiolarians) assessed by high-throughput sequencing. PLoS One 9:e104297. https://doi.org/10.1371/journal.pone.0104297.

19. Weber AA-T, Pawlowski J. 2014. Wide occurrence of SSU rDNA intragenomic polymorphism in foraminifera and its implications for molecular species identification. Protist 165:645-661. https://doi.org/10.1016/j.protis.2014.07.006.

20. Kudryavtsev A, Gladkikh A. 2017. Two new species of *Ripella* (Amoebozoa, Vannellida) and unusual intragenomic variability in the SSU rRNA gene of this genus. Eur J Protistol 61:92-106. https://doi.org/10.1016/j.ejop.2017.09.003.

21. Wang C, Zhang T, Wang Y, Katz LA, Gao F, Song W. 2017. Disentangling sources of

variation in SSU rDNA sequences from single cell analyses of ciliates: Impact of copy number variation and experimental error. Proc R Soc Lond B Biol Sci 284:20170425. https://doi.org/10.1098/rspb.2017.0425.

22. Gunderson JH, Sogin ML, Wollett G, Hollingdale M, de la Cruz VF, Waters AP, McCutchan TF. 1987. Structurally distinct, stage-specific ribosomes occur in Plasmodium. Science 238:933. https://doi.org/10.1126/science.3672135.

23. López-López A, Benlloch S, Bonfá M, Rodríguez-Valera F, Mira A. 2007. Intragenomic 16S rDNA divergence in *Haloarcula marismortui* Is an adaptation to different temperatures. J Mol Evol 65:687-696. https://doi.org/10.1007/s00239-007-9047-3.

24. Genuth NR, Barna M. 2018. The discovery of ribosome heterogeneity and its implications for gene regulation and organismal life. Mol Cell 71:364-374. https://doi.org/10.1016/j.molcel.2018.07.018.

25. Kurylo CM, Parks MM, Juette MF, Zinshteyn B, Altman RB, Thibado JK, Vincent CT, Blanchard SC. 2018. Endogenous rRNA sequence variation can regulate stress response gene expression and phenotype. Cell Rep 25:236-248.e6. https://doi.org/10.1016/j.celrep.2018.08.093.

26. Stout JD. 1955. Environmental factors affecting the life history of three soil species of *Colpoda* (Ciliata). Trans Roy Soc New Zealand 82:1165-1188. https://doi.org/.

27. Müller H, Achilles-Day UEM, Day JG. 2010. Tolerance of the resting cysts of *Colpoda inflata* (Ciliophora, Colpodea) and *Meseres corlissi* (Ciliophora, Spirotrichea) to desiccation and freezing. Eur J Protistol 46:133-142. https://doi.org/10.1016/j.ejop.2009.12.004.

28. Omar A, Zhang Q, Zou S, Gong J. 2017. Morphology and phylogeny of the soil ciliate *Metopus yantaiensis* n. sp. (Ciliophora, Metopida), with identification of the intracellular bacteria. J Eukaryot Microbiol 64:792-805. https://doi.org/10.1111/jeu.12411.

29. Wilbert N. 1975. Eine verbesserte technik der protargo-limpragnation fur ciliaten. Mikrokosmos 64:171-179.

30. Warren A, Patterson DJ, Dunthorn M, Clamp JC, Achilles-Day UEM, Aescht E, Al-Farraj SA, Al-Quraishy S, Al-Rasheid K, Carr M, Day JG, Dellinger M, El-Serehy HA, Fan Y, Gao F, Gao S, Gong J, Gupta R, Hu X, Kamra K, Langlois G, Lin X, Lipscomb D, Lobban CS, Luporini P, Lynn DH, Ma H, Macek M, Mackenzie-Dodds J, Makhija S, Mansergh RI,

Martín-Cereceda M, McMiller N, Montagnes DJS, Nikolaeva S, Ong'ondo GO, Pérez-Uz B, Purushothaman J, Quintela-Alonso P, Rotterová J, Santoferrara L, Shao C, Shen Z, Shi X, Song W, Stoeck T, La Terza A, Vallesi A, Wang M, Weisse T, et al. 2017. Beyond the "Code": A guide to the description and documentation of biodiversity in ciliated protists (Alveolata, Ciliophora). J Eukaryot Microbiol 64:539-554. https://doi.org/10.1111/jeu.12391.

32. Zhu F, Massana R, Not F, Marie D, Vaulot D. 2005. Mapping of picoeucaryotes in marine ecosystems with quantitative PCR of the 18S rRNA gene. FEMS Microbiol Ecol 52:79-92. https://doi.org/10.1016/j.femsec.2004.10.006.

36. Stoeck T, Bass D, Nebel M, Christen R, Jones MDM, Breiner H-W, Richards TA. 2010. Multiple marker parallel tag environmental DNA sequencing reveals a highly complex eukaryotic community in marine anoxic water. Mol Ecol 19:21-31. https://doi.org/10.1111/j.1365-294X.2009.04480.x.

37. Díez B, Pedrós-Alió C, Marsh TL, Massana R. 2001. Application of denaturing gradient gel electrophoresis (DGGE) to study the diversity of marine picoeukaryotic assemblages and comparison of DGGE with other molecular techniques. Appl Environ Microbiol 67:2942-2951. https://doi.org/10.1128/aem.67.7.2942-2951.2001.

38. Dawson SC, Pace NR. 2002. Novel kingdom-level eukaryotic diversity in anoxic environments. Proc Natl Acad Sci U S A 99:8324. https://doi.org/10.1073/pnas.062169599.

39. Schmieder R, Edwards R. 2011. Quality control and preprocessing of metagenomic datasets. Bioinformatics 27:863-864. https://doi.org/10.1093/bioinformatics/btr026.

40. Caporaso JG, Kuczynski J, Stombaugh J, Bittinger K, Bushman FD, Costello EK, Fierer N, Peña AG, Goodrich JK, Gordon JI, Huttley GA, Kelley ST, Knights D, Koenig JE, Ley RE, Lozupone CA, McDonald D, Muegge BD, Pirrung M, Reeder J, Sevinsky JR, Turnbaugh PJ, Walters WA, Widmann J, Yatsunenko T, Zaneveld J, Knight R. 2010. QIIME allows analysis of high-throughput community sequencing data. Nat Methods 7:335-336. https://doi.org/10.1038/nmeth.f.303.

41. Schloss PD, Westcott SL, Ryabin T, Hall JR, Hartmann M, Hollister EB, Lesniewski RA, Oakley BB, Parks DH, Robinson CJ, Sahl JW, Stres B, Thallinger GG, Van Horn DJ, Weber CF. 2009. Introducing mothur: Open-source, platform-independent, community-supported

software for describing and comparing microbial communities. Appl Environ Microbiol 75:7537. https://doi.org/10.1128/AEM.01541-09.

42. Edgar RC. 2010. Search and clustering orders of magnitude faster than BLAST. Bioinformatics 26:2460-2461. https://doi.org/10.1093/bioinformatics/btq461.

43. Li H, Durbin R. 2009. Fast and accurate short read alignment with Burrows–Wheeler transform. Bioinformatics 25:1754-1760. https://doi.org/10.1093/bioinformatics/btp324.

44. Li H, Handsaker B, Wysoker A, Fennell T, Ruan J, Homer N, Marth G, Abecasis G, Durbin R, Genome Project Data Processing S. 2009. The sequence alignment/map format and SAMtools. Bioinformatics 25:2078-2079. https://doi.org/10.1093/bioinformatics/btp352.

45. Anderson DM, Lindquist NL. 1985. Time-course measurements of phosphorus depletion and cyst formation in the dinoflagellate *Gonyaulax tamarensis* Lebour. J Exp Mar Bio Ecol 86:1-13. https://doi.org/10.1016/0022-0981(85)90039-5.

46. Pérez-uz B, Guinea A. 2001. Morphology and infraciliature of a marine Scuticociliate with a polymorphic life cycle: *Urocryptum tortum* n. gen., n. comb. J Eukaryot Microbiol 48:338-347. https://doi.org/10.1111/j.1550-7408.2001.tb00323.x.

47. Jorgensen P, Edgington NP, Schneider BL, Rupeš I, Tyers M, Futcher B. 2007. The size of the nucleus increases as yeast cells grow. Mol Biol Cell 18:3523-3532. https://doi.org/10.1091/mbc.e06-10-0973.

48. Neumann FR, Nurse P. 2007. Nuclear size control in fission yeast. J Cell Biol 179:593-600. https://doi.org/10.1083/jcb.200708054.

49. Rogerson A, Butler HG, Thomason JC. 1994. Estimation of amoeba cell volume from nuclear diameter and its application to studies in protozoan ecology. Hydrobiologia 284:229-234. https://doi.org/10.1007/BF00006692.

50. Jevtić P, Levy DL. 2015. Nuclear size scaling during *Xenopus* early development contributes to midblastula transition timing. Curr Biol 25:45-52. https://doi.org/10.1016/j.cub.2014.10.051.

51. Reber S, Goehring NW. 2015. Intracellular scaling mechanisms. Cold Spring Harb Perspect Biol 7. https://doi.org/10.1101/cshperspect.a019067.

52. Wang Y, Wang C, Jiang Y, Katz LA, Gao F, Yan Y. 2019. Further analyses of variation of ribosome DNA copy number and polymorphism in ciliates provide insights relevant to

studies of both molecular ecology and phylogeny. Sci China Life Sci 62:203-214. https://doi.org/10.1007/s11427-018-9422-5.

53. Engberg J, Pearlman RE. 1972. The amount of ribosomal RNA genes in *Tetrahymena pyriformis* in different physiological states. Eur J Biochem 26:393-400. https://doi.org/10.1111/j.1432-1033.1972.tb01779.x.

54. Main CR, Doll C, Bianco C, Greenfield DI, Coyne KJ. 2014. Effects of growth phase, diel cycle and macronutrient stress on the quantification of *Heterosigma akashiwo* using qPCR and SHA. Harmful Algae 37:92-99. https://doi.org/10.1016/j.hal.2014.05.014.

55. Galluzzi L, Bertozzini E, Penna A, Perini F, Garcés E, Magnani M. 2010. Analysis of rRNA gene content in the Mediterranean dinoflagellate *Alexandrium catenella* and *Alexandrium taylori*: implications for the quantitative real-time PCR-based monitoring methods. J Appl Phycol 22:1-9. https://doi.org/10.1007/s10811-009-9411-3.

56. Eckford-Soper LK, Daugbjerg N. 2016. A quantitative real-time PCR assay for identification and enumeration of the occasionally co-occurring ichthyotoxic *Pseudochattonella farcimen* and *P. verruculosa* (Dictyochophyceae) and analysis of variation in gene copy numbers during the growth phase of single and mixed cultures. J Phycol 52:174-183. https://doi.org/10.1111/jpy.12389.

57. Nishimura T, Hariganeya N, Tawong W, Sakanari H, Yamaguchi H, Adachi M. 2016. Quantitative PCR assay for detection and enumeration of ciguatera-causing dinoflagellate *Gambierdiscus* spp. (Gonyaulacales) in coastal areas of Japan. Harmful Algae 52:11-22. https://doi.org/10.1016/j.hal.2015.11.018.

58. Gillooly JF, Allen AP, Brown JH, Elser JJ, del Rio CM, Savage VM, West GB, Woodruff WH, Woods HA. 2005. The metabolic basis of whole-organism RNA and phosphorus content. Proc Natl Acad Sci U S A 102:11923. https://doi.org/10.1073/pnas.0504756102.

59. Weber AAT, Pawlowski J. 2013. Can abundance of protists be inferred from sequence data: A case study of Foraminifera. PLoS One 8:e56739. https://doi.org/10.1371/journal.pone.0056739.

60. Prescott DM. 1994. The DNA of ciliated protozoa. Microbiol Rev 58:233. https://doi.org/10.1128/mmbr.58.2.233-267.1994.

61. Cavalier-Smith T. 1978. Nuclear volume control by nucleoskeletal DNA, selection for cell

volume and cell growth rate, and the solution of the DNA C-value paradox. J Cell Sci 34:247.

62. Elser JJ, Sterner RW, Gorokhova E, Fagan WF, Markow TA, Cotner JB, Harrison JF, Hobbie SE, Odell GM, Weider LW. 2000. Biological stoichiometry from genes to ecosystems. Ecol Lett 3:540-550. https://doi.org/10.1111/j.1461-0248.2000.00185.x.

63. Weiss RL, Kukora JR, Adams J. 1975. The relationship between enzyme activity, cell geometry, and fitness in *Saccharomyces cerevisiae*. Proc Natl Acad Sci U S A 72:794-798. https://doi.org/10.1073/pnas.72.3.794.

64. Mable BK, Otto SP. 2001. Masking and purging mutations following EMS treatment in haploid, diploid and tetraploid yeast (*Saccharomyces cerevisiae*). Genet Res 77:9-26. https://doi.org/10.1017/S0016672300004821.

65. Hessen DO, Jeyasingh PD, Neiman M, Weider LJ. 2010. Genome streamlining and the elemental costs of growth. Trends Ecol Evol 25:75-80. https://doi.org/10.1016/j.tree.2009.08.004.

66. Zhao F, Filker S, Xu K, Li J, Zhou T, Huang P. 2019. Effects of intragenomic polymorphism in the SSU rRNA gene on estimating marine microeukaryotic diversity: A test for ciliates using single-cell high-throughput DNA sequencing. Limnol Oceanogr Methods 17:533-543. https://doi.org/10.1002/lom3.10330.

67. Alverson AJ, Kolnick L. 2005. Intragenomic nucleotide polymorphism among small subunit (18S) rDNA paralogs in the diatom genus *Skeletonema* (Bacillariophyta). J Phycol 41:1248-1257. https://doi.org/10.1111/j.1529-8817.2005.00136.x.

68. Caron DA, Hu SK. 2019. Are we overestimating protistan diversity in nature? Trends Microbiol 27:197-205. https://doi.org/10.1016/j.tim.2018.10.009.

69. Song W, Joo M, Yeom J-H, Shin E, Lee M, Choi H-K, Hwang J, Kim Y-I, Seo R, Lee JE, Moore CJ, Kim Y-H, Eyun S-i, Hahn Y, Bae J, Lee K. 2019. Divergent rRNAs as regulators of gene expression at the ribosome level. Nat Microbiol 4:515-526. https://doi.org/10.1038/s41564-018-0341-1.

70. Van de Peer Y, Mizrachi E, Marchal K. 2017. The evolutionary significance of polyploidy. Nat Rev Genet 18:411-424. https://doi.org/10.1038/nrg.2017.26.

71. Mentewab AB, Jacobsen MJ, Flowers RA. 2011. Incomplete homogenization of 18S

ribosomal DNA coding regions in *Arabidopsis thaliana*. BMC Res Notes 4:93. https://doi.org/10.1186/1756-0500-4-93.

72. Stoltzfus A, Norris RW. 2015. On the causes of evolutionary transition: Transversion bias. Mol Biol Evol 33:595-602. https://doi.org/10.1093/molbev/msv274.

73. Long H, Doak TG, Lynch M. 2018. Limited mutation-rate variation within the *Paramecium aurelia* species complex. G3: Genes, Genomes, Genetics 8:2523-2526. https://doi.org/10.1534/g3.118.200420.

74. Benítez L, Gutiérrez JC. 1997. Encystment - specific mRNA is accumulated in the resting cysts of the ciliate *Colpoda inflata*. IUBMB Life 41:1137-1141. https://doi.org/10.1080/15216549700202221.

75. Palacios G, Martin-Gonzalez A, Gutierrez JC. 1994. Macronuclear DNA demethylation is involved in the encystment process of the ciliate *Colpoda inflata*. Cell Biol Int 18:201-206. https://doi.org/10.1006/cbir.1994.1062.

Figure legends

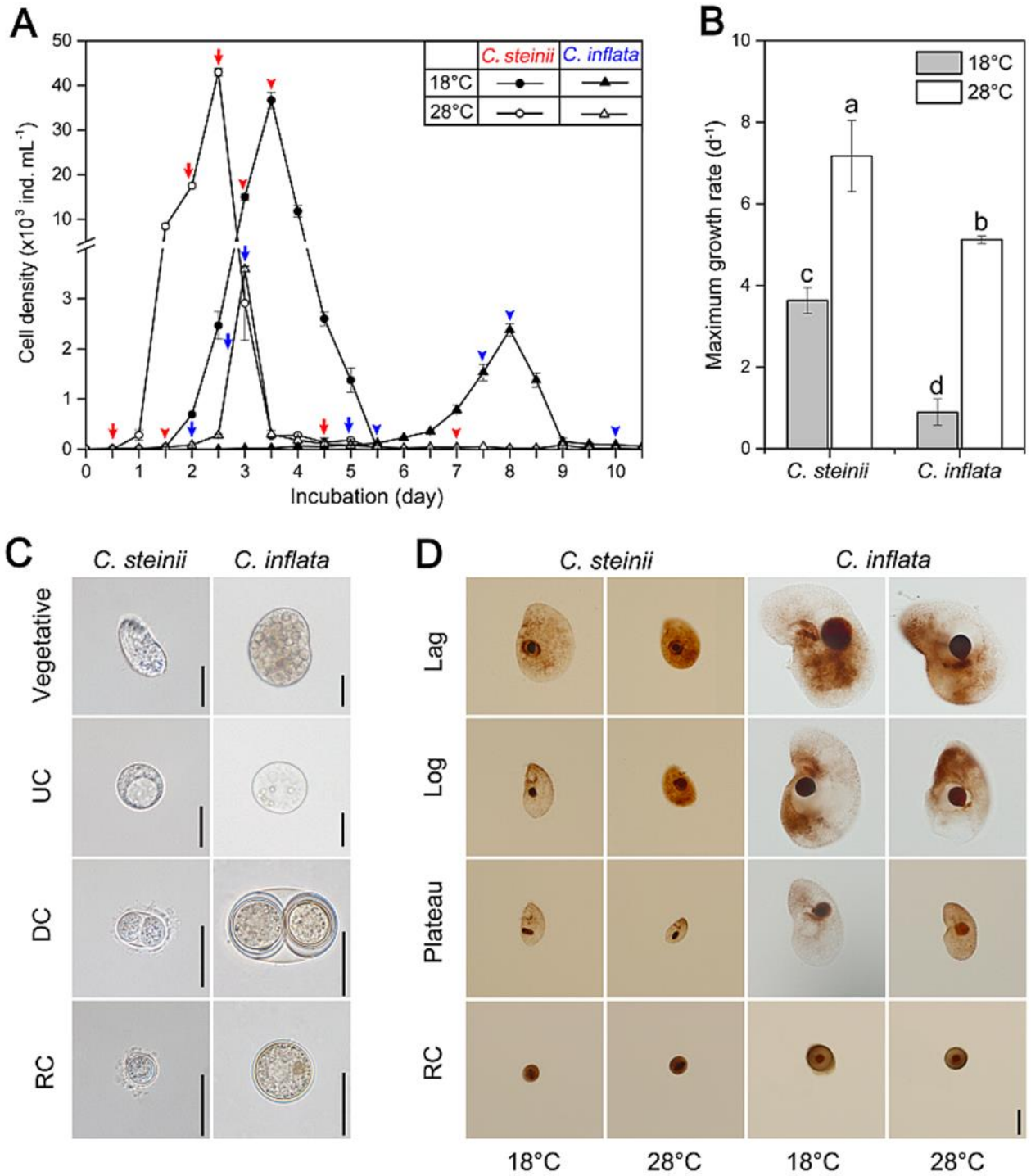

Figure 1. Growth and morphology of the soil ciliates *Colpoda steinii* and *C. inflata* reared at 18 ℃ and 28 ℃. **(A)** Growth curves of *C. steinii* (arrows and arrowheads in red) and *C. inflata* (arrows and arrowheads in blue), depicting cell isolation time-points at lag, log, plateau and resting cyst phases. **(B)** Maximum growth rates of cells at log phase. Treatments not sharing common letters indicate significant differences ($P < 0.05$). **(C)** Morphology of vegetative cells, unstable cysts (UC), dividing cysts (DC) and resting cysts (RC) from life. **(D)** Microphotographs of fixed specimens after protargol impregnation. Cell and macronuclear sizes across life-cycle stages, temperatures and species. Scale bars = 20 μm.

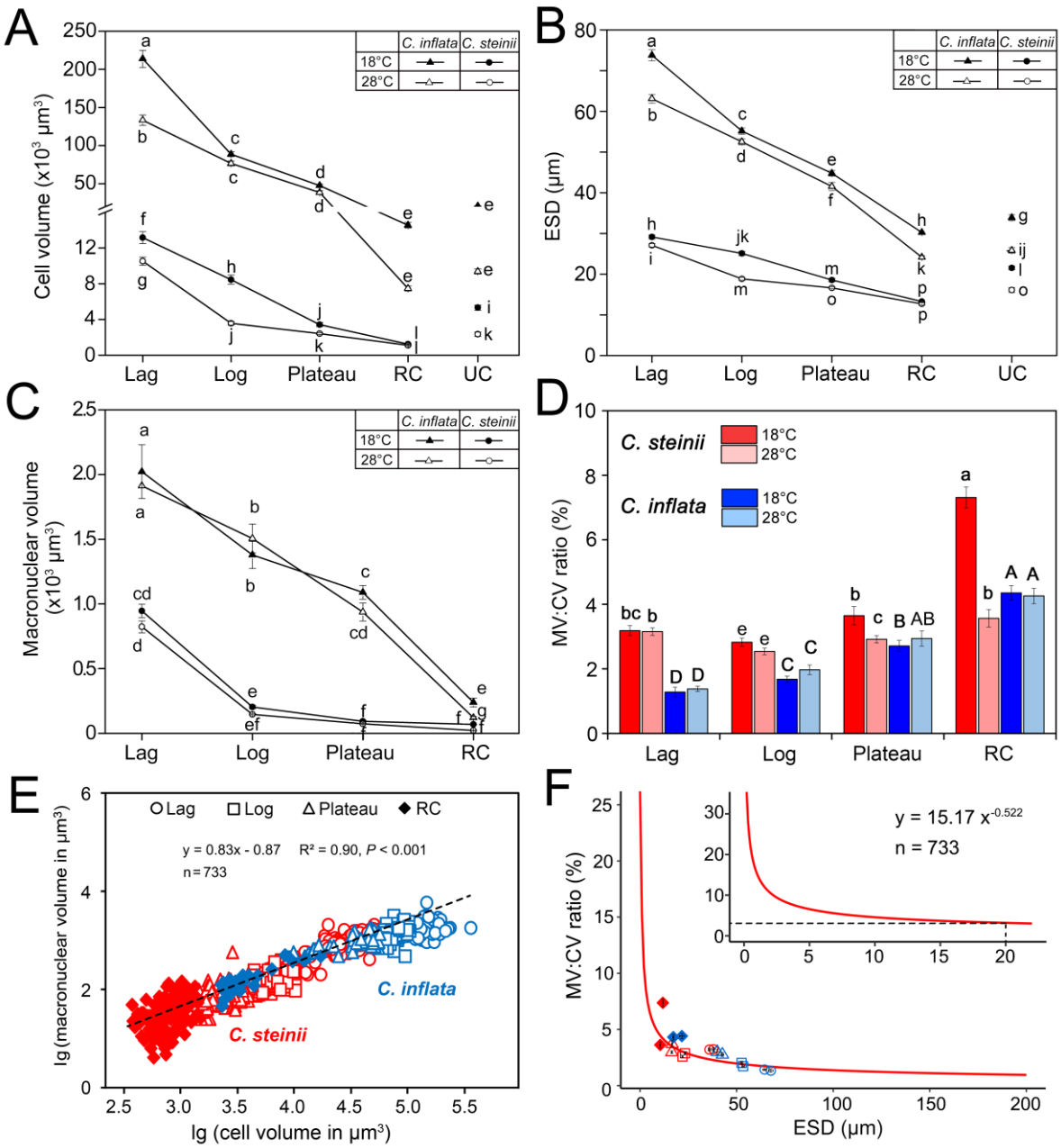

Figure 2. Variation in phenotypic traits of *Colpoda steinii* and *C. inflata* across life-cycle stages and at two temperatures. Unconnected points in line graph panels indicate unstable cysts. (**A**) Cell volume progressively decreased from lag to resting cyst phases. In general, unstable cysts were larger than resting cysts. Cells at a given growth phase were consistently larger at 18 ℃ than at 28 ℃. (**B**) Equivalent spherical diameter (ESD) progressively decreased from lag to resting cyst phases. **(C)** Macronuclear volume changed similarly to cell volume across stages, but was mostly not significant between the two temperatures. **(D)** Ratio of macronuclear to cell volume (MV:CV) across life-cycle stages. **(E)** A linear log-log relationship between macronuclear and cell volumes across life-cycle stages. **(F)** A modeled scaling relationship between MV:CV ratio and ESD. Nucleocytoplasmic ratio varies dramatically in small cells [e.g., pico- (< 2 µm) and nano-sized protists (2 ~ 20 µm)], but changes only slightly in large cells [e.g., microplanktons (20 ~ 200 µm)]. Non-sharing of common letters indicates significant differences ($P < 0.05$). RC = resting cyst; UC = unstable cyst.

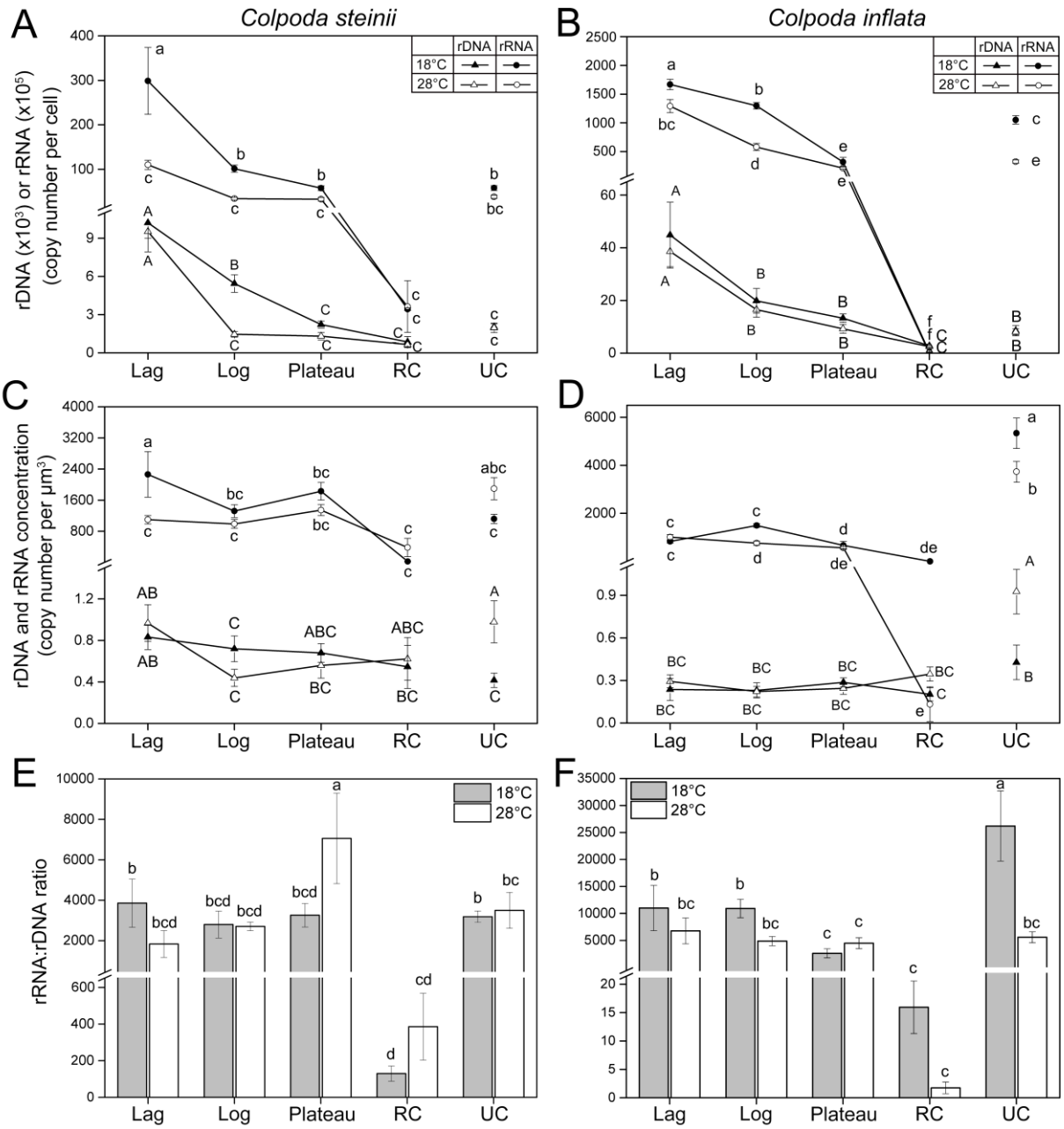

Figure 3. Variation in ribotypic traits of *Colpoda steinii* (A, C and E) and *C. inflata* (B, D and F) across lag, log, plateau, resting (RC) and unstable cyst (UC) stages and at two culturing temperatures. Unconnected points in line graph panels indicate unstable cysts. (**A, B**) Single-cell 18S rDNA and rRNA copy numbers progressively and significantly decreased from lag to RC phase. Cells in the UC stage generally had similar amounts of rDNA and rRNA as the vegetative cells in plateau phase. (**C, D**) Cellular concentrations of 18S rDNA and rRNA molecules were generally stable across lag, log, plateau and UC phases, but rRNA concentrations were significantly reduced in resting cysts of both species. (**E, F**) Copy number ratios of rRNA to rDNA in single cells were significantly lower in resting cysts of both species. The ratio was consistent in all other life-cycle phases of *C. steinii*, and lower in plateau and unstable cystic phases of *C. inflata* (relative to its log phase). Bars represent standard errors. Treatments not sharing common letters indicate significant differences ($P < 0.05$).

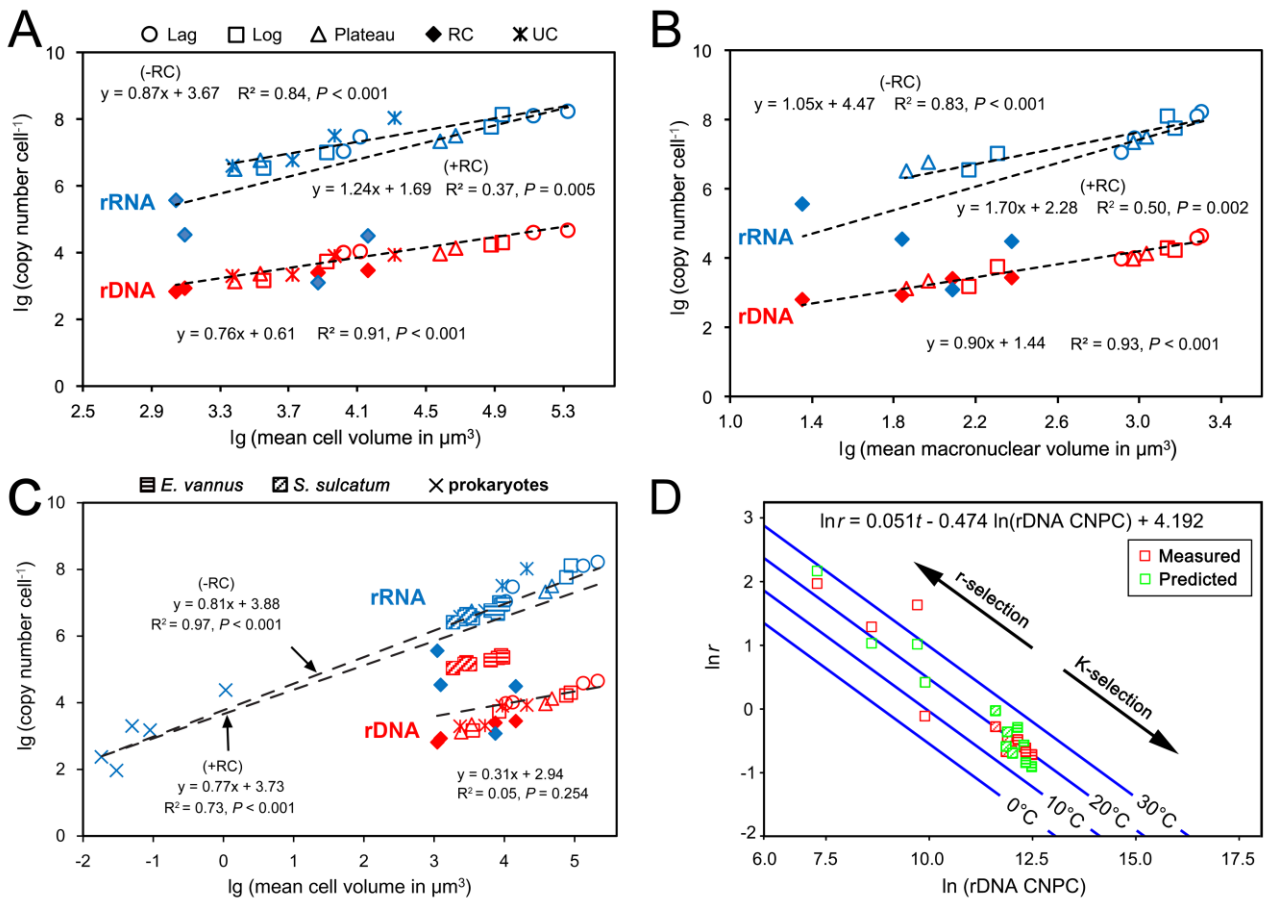

Figure 4. Scaling relationships among ribotypic traits, growth rate, and cellular attributes. **(A, B)** The per-cell rDNA and rRNA copy numbers (CNs) in two *Colpoda* species across life-cycle stages was significantly related to cell volume **(A)** and macronuclear volume **(B)**. Nevertheless, the rRNA CNs appeared to be much lower than similarly sized vegetative cells or unstable cysts, such that the coefficients of determination (R^2) of regressions were much lower with resting cysts being taken into account (+RC) than without (-RC). (**C**) Scaling relationships based on a combined dataset consisting of two *Colpoda* species (present study), *Euplotes vannus* and *Strombidium sulcatum*, and five prokaryotic species (Fu and Gong 2017). The per-cell rRNA CNs are better predicted using cell volume when resting cysts (indicated by four symbols of solid diamond in blue) are excluded from the regression analysis (-RC). The rDNA CNs of *E. vannus* and *S. sulcatum* were much higher than those of *Colpoda* cells with similar size ranges, suggesting that rDNA CN and CV relationship may be conserved among closely related taxa, but becomes inconsistent among distant taxa. (**D**) Maximum growth rates (*r*) of *Colpoda steinii*, *C. inflata*, *E. vannus* and *S. sulcatum* can be well predicted by rDNA CN per cell (CNPC) and temperature (*t*). Lines in blue denote predicted growth rates at 0, 10, 20 and 30 ℃. The amount of rDNA copies in genomes is inversely related to the growth potential of the cell, which might underline r- and K-selection of these organisms. RC = resting cysts; UC = unstable cysts.

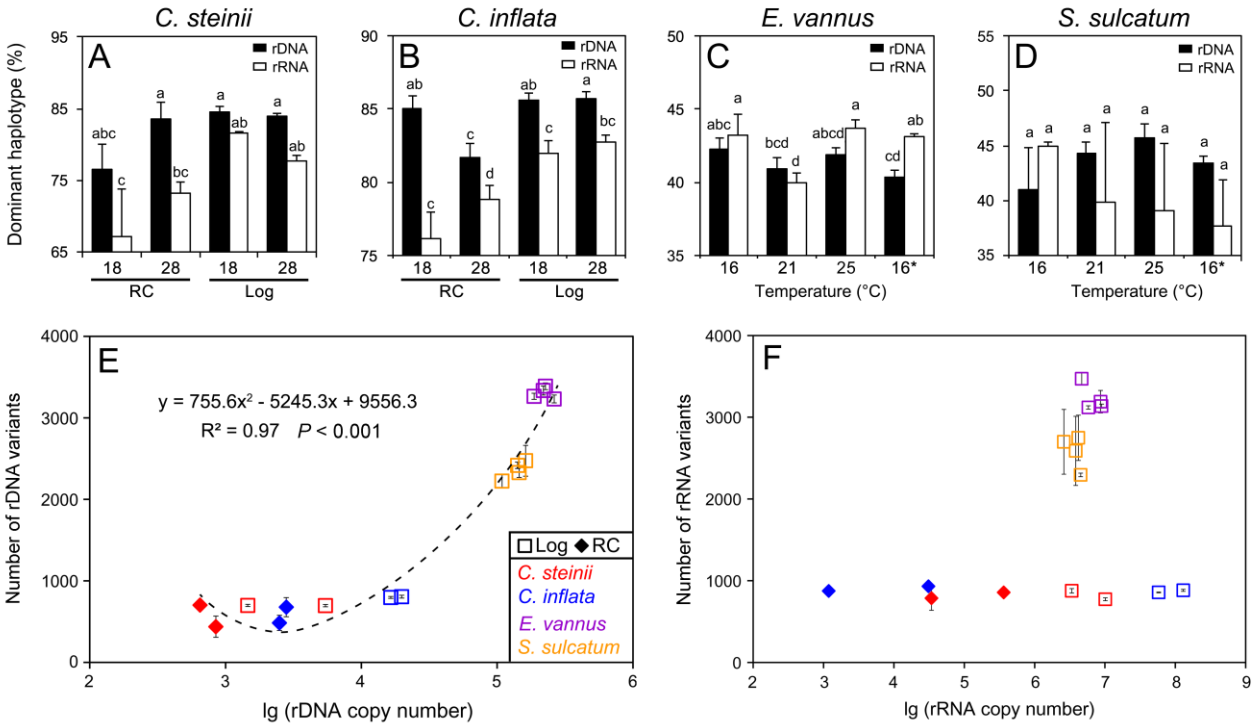

Figure 5. Variation in ribotypic traits based on intra-individual sequence polymorphisms in four ciliate species. **(A - D)** Proportions of the most dominant haplotypes in single-cell rDNA and rRNA pools, showing the differences between resting cysts (RC) and log-phase vegetative cells (Log), and among different culturing temperatures (in ℃). **(E, F)** The haplotype richness of rDNA depended on rDNA number within a cell **(E)**, but the haplotype richness of their transcripts was relatively stable and taxon-dependent, regardless of changes in cellular rRNA content **(F)**. Two treatments not sharing common letters indicate significant differences (multiple pairwise comparisons, $P < 0.05$). Log = cells in log phase of growth; RC = resting cysts.

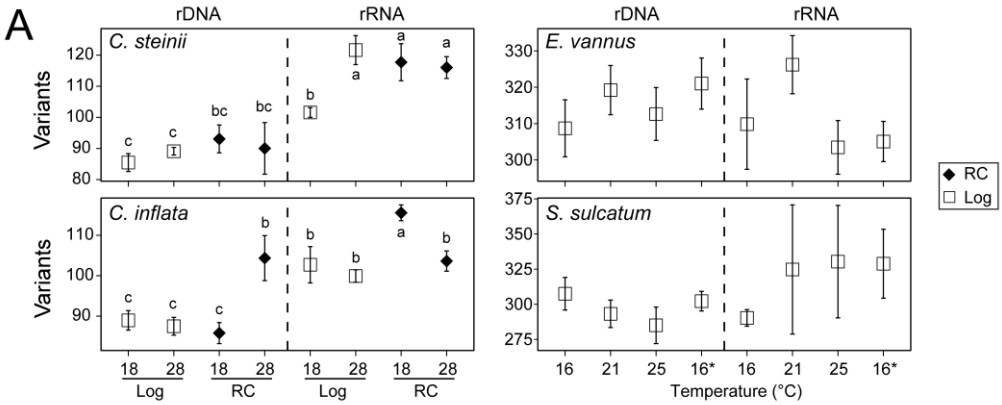

B

OTU cutoff (%)			99	98	97	96	95	94	93	92	91	90
C. steinii rDNA	RC	18	3.7 ± 0.2^{ab}	2.6 ± 0.2	2.0 ± 0.0^{ab}	2.0 ± 0.0^{b}	2.0 ± 0.0^{ab}	2.0 ± 0.0	2.0 ± 0.0^{a}	2.0 ± 0.0^{a}	1.9 ± 0.1^{a}	1
		28	3.6 ± 0.8^{ab}	2.5 ± 0.2	2.1 ± 0.1^{a}	2.1 ± 0.1^{a}	2.0 ± 0.0^{ab}	2.0 ± 0.0	1.6 ± 0.2^{bc}	1.5 ± 0.2^{b}	1.5 ± 0.3^{ab}	1
	Log	18	3.2 ± 0.1^{b}	2.4 ± 0.1	2.1 ± 0.0^{a}	2.1 ± 0.0^{a}	2.0 ± 0.0^{ab}	2.0 ± 0.0	1.4 ± 0.0^{bc}	1.4 ± 0.0^{b}	1.4 ± 0.1^{b}	1
		28	3.1 ± 0.4^{b}	2.4 ± 0.2	2.0 ± 0.0^{b}	2.0 ± 0.1^{b}	2.0 ± 0.0^{b}	1.9 ± 0.1	1.6 ± 0.1^{bc}	1.4 ± 0.1^{b}	1.4 ± 0.0^{b}	1
C. steinii rRNA	RC	18	4.7 ± 0.7^{a}	2.7 ± 0.1	2.0 ± 0.0^{ab}	2.0 ± 0.0^{ab}	2.0 ± 0.0^{ab}	2.0 ± 0.0	1.8 ± 0.2^{ab}	1.7 ± 0.2^{ab}	1.8 ± 0.2^{ab}	1
		28	4.5 ± 0.5^{a}	2.6 ± 0.1	2.0 ± 0.0^{ab}	2.0 ± 0.0^{ab}	2.0 ± 0.0^{ab}	2.0 ± 0.0	1.9 ± 0.1^{ab}	1.9 ± 0.0^{a}	1.9 ± 0.1^{a}	1
	Log	18	3.2 ± 0.1^{b}	2.5 ± 0.1	2.0 ± 0.0^{ab}	2.0 ± 0.0^{ab}	2.0 ± 0.0^{a}	2.0 ± 0.0	1.5 ± 0.1^{c}	1.5 ± 0.1^{b}	1.5 ± 0.1^{b}	1
		28	3.7 ± 0.1^{ab}	2.4 ± 0.1	2.1 ± 0.0^{ab}	2.1 ± 0.0^{ab}	2.0 ± 0.0^{a}	2.0 ± 0.0	1.5 ± 0.1^{c}	1.5 ± 0.1^{b}	1.5 ± 0.1^{b}	1
C. inflata rDNA	RC	18	1.8 ± 0.3^{c}	1.2 ± 0.2^{c}	1.2 ± 0.2^{b}	1.2 ± 0.2^{b}	1^{b}	1^{b}	1^{c}	1^{c}	1	1
		28	3.1 ± 0.7^{b}	1.5 ± 0.4^{b}	1.5 ± 0.4^{b}	1.5 ± 0.4^{ab}	1.2 ± 0.2^{b}	1.2 ± 0.2^{b}	1^{c}	1^{c}	1	1
	Log	18	1.9 ± 0.3^{c}	1.1 ± 0.0^{c}	1.1 ± 0.0^{b}	1.1 ± 0.0^{b}	1^{b}	1^{b}	1^{c}	1^{c}	1	1
		28	1.5 ± 0.1^{c}	1.1 ± 0.0^{c}	1.1 ± 0.0^{b}	1.1 ± 0.0^{b}	1^{b}	1^{b}	1^{c}	1^{c}	1	1
C. inflata rRNA	RC	18	4.7 ± 0.5^{a}	2.6 ± 0.2^{a}	2.1 ± 0.3^{a}	2.1 ± 0.3^{a}	1.8 ± 0.2^{a}	1.8 ± 0.2^{a}	1.6 ± 0.2^{b}	1.5 ± 0.2^{b}	1	1
		28	3.3 ± 0.1^{b}	2.0 ± 0.0^{b}	2.0 ± 0.0^{a}	2.0 ± 0.0^{a}	2.0 ± 0.0^{a}	2.0 ± 0.0^{a}	1.9 ± 0.1^{a}	1.8 ± 0.1^{a}	1	1
	Log	18	1.9 ± 0.1^{c}	1.1 ± 0.0^{c}	1.1 ± 0.0^{b}	1.1 ± 0.0^{b}	1^{b}	1^{b}	1^{c}	1^{c}	1	1
		28	1.8 ± 0.0^{c}	1.1 ± 0.1^{c}	1.2 ± 0.1^{b}	1.1 ± 0.0^{b}	1.2 ± 0.1^{b}	1.1 ± 0.0^{b}	1^{c}	1^{c}	1	1
E. vannus rDNA	Log	16	1.1 ± 0.0	1^{ab}	1	1^{b}	1^{b}	1	1	1	1	1
		21	1	1^{ab}	1	1^{b}	1^{ab}	1	1	1	1	1
		25	1.3 ± 0.2	1.4 ± 0.2^{a}	1.4 ± 0.2	1.4 ± 0.2^{a}	1.3 ± 0.1^{a}	1.1 ± 0.1	1.1 ± 0.1	1	1	1
		16*	1.2 ± 0.2	1.2 ± 0.2^{ab}	1.3 ± 0.3	1.1 ± 0.1^{ab}	1.2 ± 0.2^{ab}	1.1 ± 0.1	1.1 ± 0.1	1	1	1
E. vannus rRNA	Log	16	1	1.1 ± 0.1^{ab}	1	1^{b}	1^{b}	1	1	1	1	1
		21	2 ± 0.9	1.3 ± 0.3^{ab}	1.2 ± 0.2	1.1 ± 0.1^{ab}	1^{ab}	1	1	1	1	1
		25	1	1^{b}	1	1^{b}	1^{b}	1	1	1	1	1
		16*	1.1 ± 0.0	1^{b}	1	1^{b}	1^{b}	1	1	1	1	1
S. sulcatum rDNA	Log	16	1	1	1	1	1	1	1	1	1	1
		21	1	1	1	1	1	1	1	1	1	1
		25	1.2 ± 0.2	1	1	1	1	1	1	1	1	1
		16*	1.1 ± 0.1	1	1	1	1	1	1	1	1	1
S. sulcatum rRNA	Log	16	1	1	1	1	1	1	1	1	1	1
		21	1.5 ± 0.4	1	1	1	1	1	1	1	1	1
		25	1.6 ± 0.6	1	1	1	1	1	1	1	1	1
		16*	1.2 ± 0.0	1	1	1	1	1	1	1	1	1

Figure 6. Variation in the numbers of variants and OTUs in rDNA and rRNA (cDNA) pools of single cells of four ciliated protists. **(A)** Comparisons of variant numbers in a single resting cyst (RC) and log-phase cell (Log) of *Colpoda steinii* and *C. inflata* at 18 ℃ and 28 ℃. **(B)** Comparisons of variant numbers in a single log-phase cell of *Euplotes vannus* and *Strombidium sulcatum* at four temperatures. The OTUs were defined at a sequence similarity threshold ranging from 90% to 99%. At the threshold of 97% (the typical OTU definition threshold applied in metabarcoding studies), the single cells of these species had on average > 1 (up to 2.8) OTU(s), except for *S. sulcatum*. The maximum intra-individual rDNA and rRNA sequence differences of the four species ranged from 1% (in *S. sulcatum*) to 9% (in *C. steinii*). Singletons were not included in these analyses. Two treatments not sharing common letters indicate significant differences (multiple pairwise comparisons, $P < 0.05$).

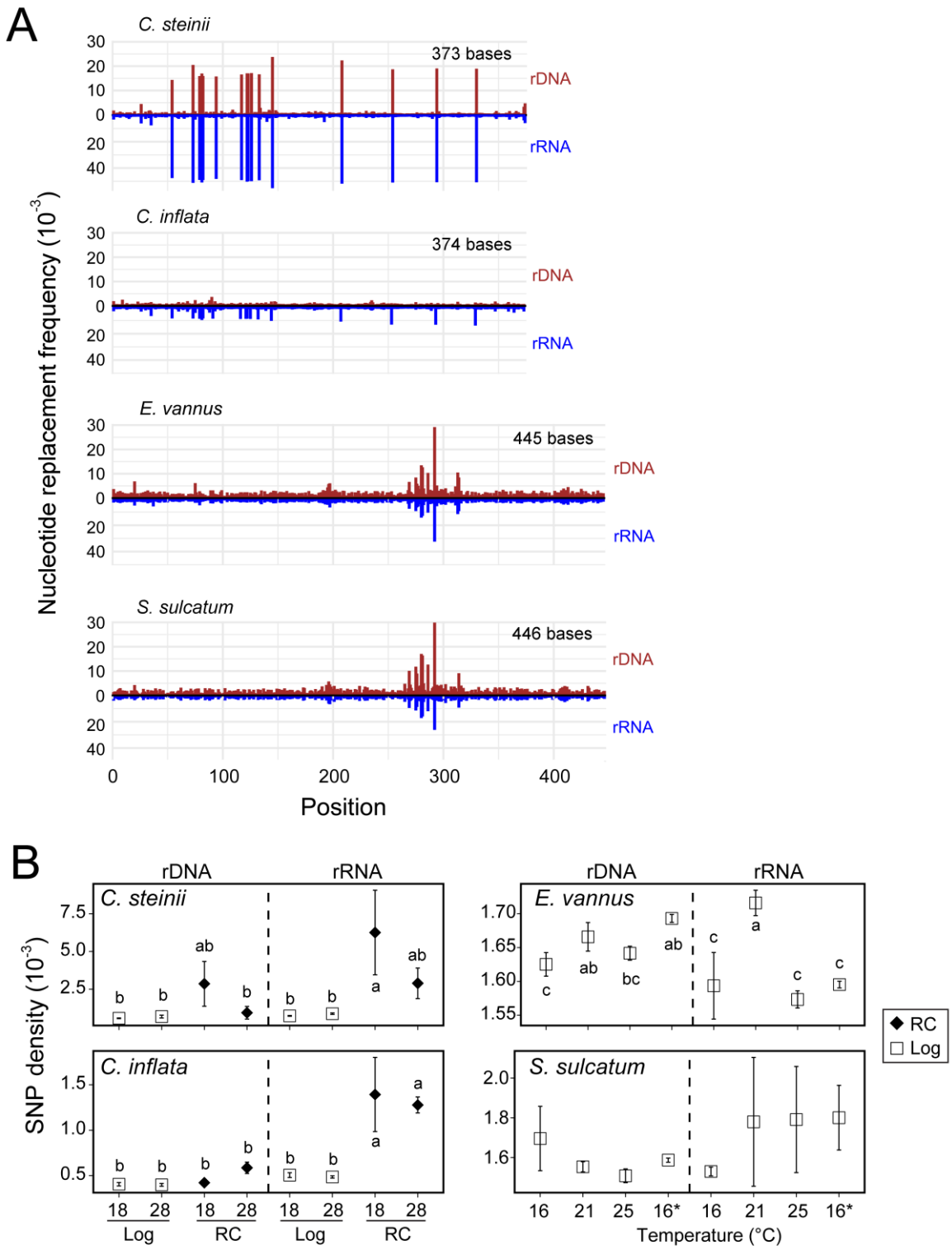

Figure 7. Single nucleotide polymorphisms in rDNA and rRNA (cDNA) fragments of four ciliate species identified using high throughput sequencing. **(A)** Nucleotide replacement frequencies were much higher at certain positions (polymorphic sites), which were consistent between rDNA and rRNA, between the two *Colpoda* species, and between *E. vannus* and *S. sulcatum*. **(B)** Comparisons of nucleotide replacement frequencies of rDNA and rRNA at log-phase cells vs. resting cysts, and at different temperatures of four ciliate species. Two treatments not sharing common letters indicate significant differences (multiple pairwise comparisons, $P < 0.05$).

				Ts(A/G)	Ts(C/T)	Tv(G/T)	Tv(T/A)	Tv(A/C)	Tv(G/C)	Ts:Tv
C. steinii	rDNA	RC	18	10.3 ± 1.3 ^{b}	43.4 ± 3.3 ^{a}	13.6 ± 0.9 ^{c}	20.6 ± 2.0 ^{ab}	2.7 ± 1.1 ^{c}	9.4 ± 1.2 ^{ab}	1.2 ± 0.2
			28	18.4 ± 3.6 ^{ab}	33.1 ± 3.6 ^{abc}	17.8 ± 2.2 ^{ab}	16.8 ± 2.0 ^{ab}	6.8 ± 1.6 ^{abc}	7.0 ± 1.4 ^{ab}	1.1 ± 0.0
		Log	18	22.4 ± 2.5 ^{a}	29.6 ± 1.1 ^{c}	19.4 ± 0.6 ^{a}	14.2 ± 0.8 ^{b}	8.9 ± 0.8 ^{a}	5.5 ± 0.5 ^{b}	1.1 ± 0.1
			28	20.0 ± 1.7 ^{a}	31.7 ± 2.1 ^{bc}	18.7 ± 0.7 ^{ab}	15.0 ± 1.3 ^{ab}	8.3 ± 1.6 ^{ab}	6.3 ± 0.6 ^{ab}	1.1 ± 0.0
	rRNA	RC	18	15.1 ± 4.2 ^{ab}	38.2 ± 2.4 ^{b}	14.0 ± 0.9 ^{c}	20.0 ± 2.6 ^{ab}	3.5 ± 1.6 ^{bc}	9.1 ± 1.6 ^{ab}	1.2 ± 0.1
			28	19.0 ± 3.8 ^{ab}	36.9 ± 2.2 ^{b}	13.4 ± 0.2 ^{c}	19.4 ± 1.6 ^{a}	2.5 ± 0.6 ^{c}	8.8 ± 1.1 ^{a}	1.3 ± 0.1
		Log	18	21.1 ± 0.8 ^{a}	32.3 ± 0.2 ^{abc}	17.1 ± 0.4 ^{b}	15.9 ± 0.5 ^{ab}	7.5 ± 0.3 ^{ab}	6.1 ± 0.4 ^{ab}	1.1 ± 0.0
			28	22.6 ± 0.6 ^{a}	32.7 ± 1.5 ^{abc}	15.2 ± 0.4 ^{c}	15.2 ± 0.4 ^{ab}	8.0 ± 0.9 ^{ab}	6.4 ± 0.2 ^{ab}	1.2 ± 0.1
C. inflata	rDNA	RC	18	32.8 ± 2.8 ^{a}	27.6 ± 1.1 ^{c}	14.1 ± 0.7	14.3 ± 1.0 ^{b}	8.3 ± 0.6 ^{ab}	2.9 ± 0.6 ^{c}	1.6 ± 0.2 ^{ab}
			28	28.1 ± 1.2 ^{a}	27.9 ± 2.5 ^{bc}	14.2 ± 1.0	16.9 ± 1.4 ^{ab}	7.9 ± 0.9 ^{ab}	5.0 ± 0.4 ^{b}	1.3 ± 0.1 ^{b}
		Log	18	30.1 ± 1.3 ^{a}	26.8 ± 1.4 ^{c}	15.9 ± 1.4	14.7 ± 0.4 ^{b}	8.3 ± 0.5 ^{a}	4.2 ± 0.9 ^{bc}	1.3 ± 0.1 ^{ab}
			28	31.4 ± 0.9 ^{a}	28.4 ± 0.7 ^{c}	14.2 ± 0.8	14.6 ± 0.5 ^{b}	7.8 ± 0.2 ^{a}	3.5 ± 0.1 ^{c}	1.5 ± 0.1 ^{ab}
	rRNA	RC	18	23.7 ± 3.6 ^{ab}	36.4 ± 1.4 ^{a}	12.4 ± 0.5	17.3 ± 1.5 ^{ab}	4.4 ± 0.5 ^{c}	5.7 ± 1.2 ^{abc}	1.5 ± 0.2 ^{ab}
			28	16.4 ± 0.4 ^{b}	39.1 ± 0.5 ^{a}	12.6 ± 0.6	20.2 ± 0.4 ^{a}	4.0 ± 0.4 ^{c}	7.6 ± 0.1 ^{a}	1.3 ± 0.0 ^{b}
		Log	18	32.0 ± 1.3 ^{a}	30.3 ± 0.9 ^{bc}	12.4 ± 1.0	14.9 ± 0.7 ^{b}	6.8 ± 0.4 ^{b}	3.7 ± 0.6 ^{bc}	1.7 ± 0.2 ^{a}
			28	31.2 ± 0.5 ^{a}	31.4 ± 0.5 ^{b}	12.6 ± 0.4	14.9 ± 0.4 ^{b}	6.7 ± 0.1 ^{b}	3.2 ± 0.1 ^{c}	1.7 ± 0.1 ^{a}
E. vannus	rDNA	Log	16	42.4 ± 1.2	32.0 ± 0.2 ^{a}	12.4 ± 0.5	6.7 ± 0.7	5.3 ± 0.3	1.2 ± 0.2	2.9 ± 0.2
			21	41.2 ± 1.2	32.5 ± 0.8 ^{a}	11.1 ± 0.9	7.2 ± 1.0	6.7 ± 1.7	1.3 ± 0.2	2.9 ± 0.3
			25	43.2 ± 1.0	31.6 ± 0.2 ^{a}	12.4 ± 0.5	6.8 ± 0.8	4.8 ± 0.5	1.2 ± 0.2	3.0 ± 0.2
			16*	42.3 ± 0.6	31.4 ± 0.5 ^{ab}	12.1 ± 0.8	6.7 ± 0.7	6.4 ± 1.1	1.2 ± 0.2	2.8 ± 0.1
	rRNA	Log	16	43.0 ± 0.9	29.6 ± 1.2 ^{ab}	12.4 ± 0.7	8.1 ± 1.1	5.5 ± 1.0	1.4 ± 0.3	2.7 ± 0.3
			21	43.4 ± 1.9	29.7 ± 1.8 ^{ab}	13.4 ± 1.8	7.1 ± 1.1	5.1 ± 1.0	1.4 ± 0.3	2.8 ± 0.5
			25	43.0 ± 0.7	29.4 ± 1.3 ^{ab}	11.9 ± 0.7	7.4 ± 0.9	7.1 ± 1.8	1.3 ± 0.2	2.7 ± 0.3
			16*	44.2 ± 1.3	29.4 ± 0.6 ^{b}	12.3 ± 0.3	7.6 ± 1.0	5.1 ± 0.6	1.3 ± 0.2	2.8 ± 0.3
S. sulcatum	rDNA	Log	16	38.6 ± 2.6	26.7 ± 3.9	17.0 ± 6.6	6.6 ± 1.5	9.6 ± 1.8	1.5 ± 0.2	2.1 ± 0.5
			21	41.5 ± 1.5	30.3 ± 0.4	13.1 ± 1.3	7.1 ± 1.2	6.4 ± 0.7	1.7 ± 0.4	2.6 ± 0.2
			25	42.4 ± 0.7	30.1 ± 0.4	13.3 ± 1.6	6.9 ± 1.1	6.0 ± 0.4	1.4 ± 0.3	2.6 ± 0.1
			16*	40.8 ± 0.9	30.3 ± 0.8	12.7 ± 2.4	7.3 ± 1.5	7.4 ± 0.7	1.6 ± 0.2	2.5 ± 0.1
	rRNA	Log	16	42.6 ± 2.1	29.3 ± 0.7	13.7 ± 0.2	7.4 ± 1.5	5.5 ± 1.0	1.4 ± 0.6	2.6 ± 0.4
			21	42.8 ± 1.1	31.2 ± 2.9	10.6 ± 2.7	8.0 ± 1.2	6.0 ± 0.5	1.4 ± 0.3	2.9 ± 0.4
			25	43.2 ± 1.8	32.1 ± 1.9	10.5 ± 2.0	7.6 ± 1.0	5.3 ± 0.7	1.4 ± 0.4	3.2 ± 0.6
			16*	39.4 ± 2.4	28.1 ± 4.8	16.4 ± 6.7	7.2 ± 1.5	7.5 ± 1.9	1.4 ± 0.2	2.4 ± 0.7

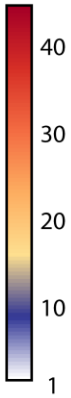

Figure 8. Distribution of transition (Ts) and transversion (Tv) categories in rDNA and rRNA (cDNA) variants in resting cyst and log-phase cells of four ciliate species reared at different temperatures. RC, resting cysts; Log, log phase cells. Two treatments not sharing common letters indicate significant differences (multiple pairwise comparisons, $P < 0.05$).

Supplementary Material

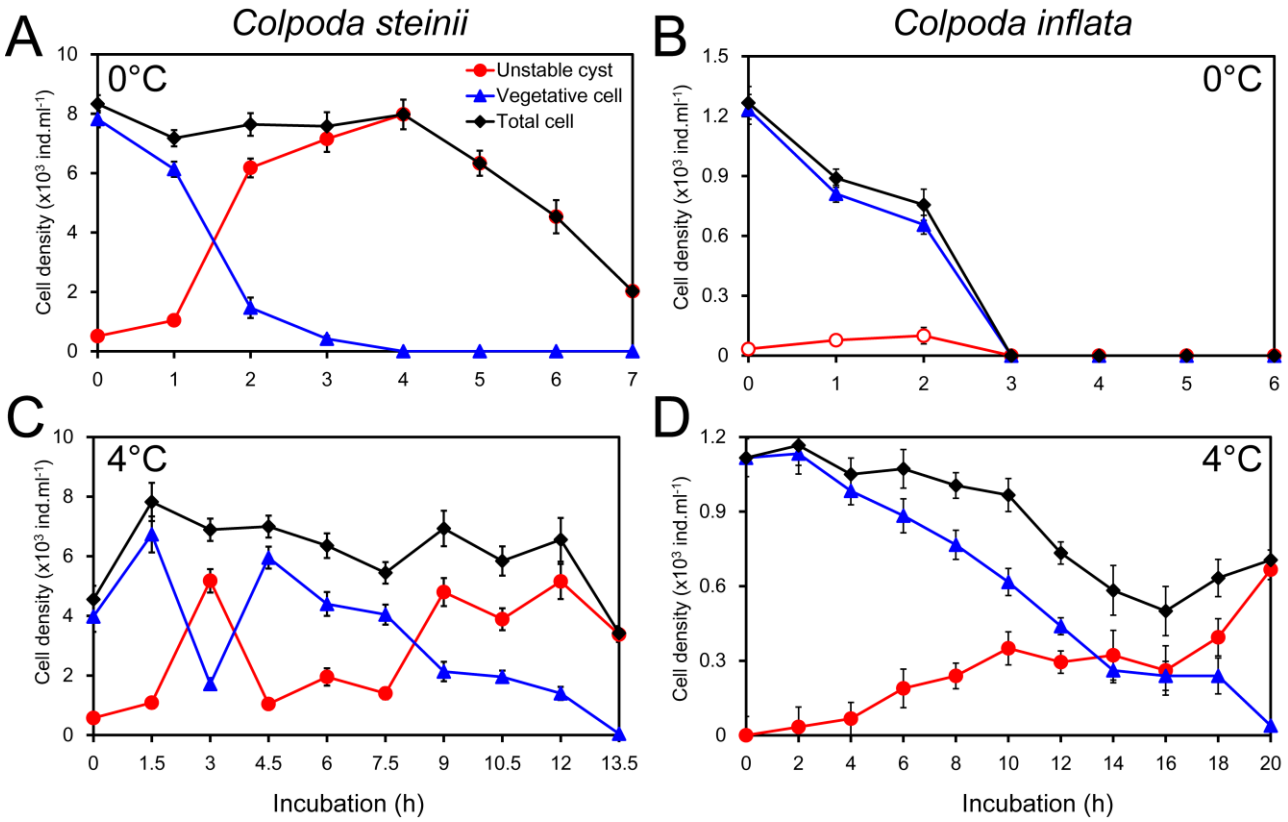

Figure S1. Chilling treatments of two *Colpoda* species induced unstable cyst formation. The chilling treatments at 0 ℃ and 4 ℃ showed that cold shock could induce formation of unstable cysts in actively growing *Colpoda* cells. Nevertheless, this effect was strongly dependent on chilling temperature and duration. Putting both *Colpoda* species at 10 ℃ did not induce formation of unstable cysts (data not shown). **(A)** Cell division of *Colpoda steinii* was completely inhibited upon ice water chilling, and nearly 100% of vegetative cells were transformed into unstable cysts in 4 hrs. Longer chilling duration led to a decrease in the number of unstable cysts. **(B)** In contrast, the population of *C. inflata* collapsed completely during ice water treatments within 3 hrs. **(C)** At 4 ℃, the small-sized *C. steinii* continued to grow and divide during the first 1.5 hrs. Afterwards, total cell abundance (= vegetative cells + unstable cysts) remained relatively stable, with approximately 76% of cells being transformed from vegetative status into unstable cysts following incubation for 9 to 12 hrs. Treating cells at 4 ℃ for a longer period of time damaged both types of cell. **(D)** Chilling at 4 ℃ completely inhibited cell division of *C. inflata*; unstable cysts progressively increased to 37% in 10 hrs, after which the number of unstable cysts remained stable for the next 8 hrs. All individuals transformed into unstable cysts in 20 hrs. Approximately, 36% of cells were lost during this incubation.